Physical modeling of atmospheric boundary layer flows

Part III: Modeling atmospheric convective boundary layer (CBL)

Evgeni Fedorovich

School of Meteorology, University of Oklahoma, Norman, USA

Outline

- **Overview of modeling techniques in laboratory studies of CBL**
- **Water tank studies of shear-free CBL by Deardorff et al.**
- **Modeling horizontally evolving CBL in the UniKa thermally stratified wind tunnel**
  - Method to generate CBL in the UniKA tunnel; scaling parameters
  - Mean flow parameters and turbulence statistics in the modeled CBL
  - Probability density distributions and turbulence spectra
  - Tracer dispersion from a point source in the horizontally evolving CBL
  - Combining wind tunnel study with numerical large eddy simulation (LES)
- **Other laboratory studies of turbulence and dispersion in CBL**
- **Summarizing remarks**

Convective boundary layer (CBL) along a heated surface

Dry (or clear) atmospheric CBL is a turbulently mixed boundary layer with the turbulence dominantly forced by heating from below and wind shear representing the secondary turbulence forcing

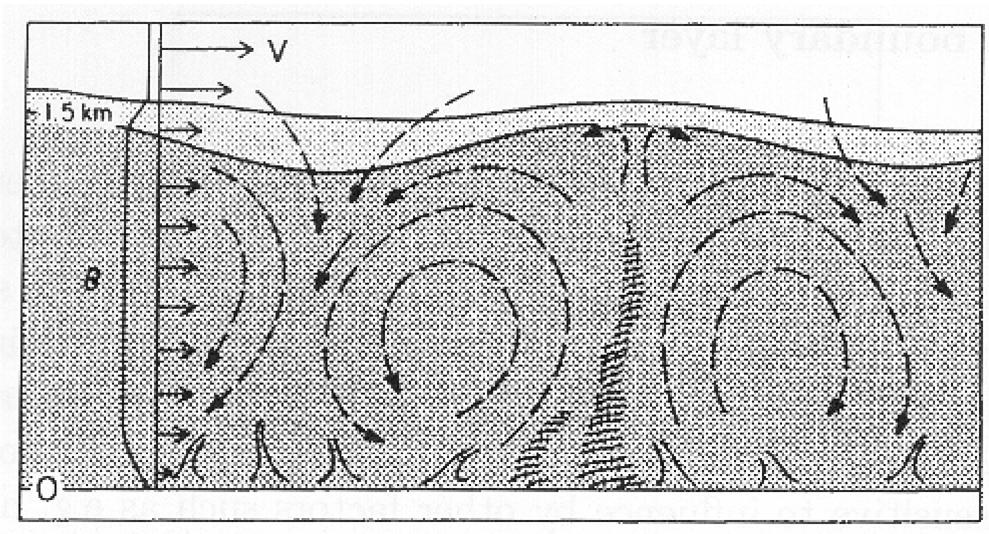

Schematic of temperature and wind fields in the atmospheric CBL (after John Wyngaard)

CBL without wind shear

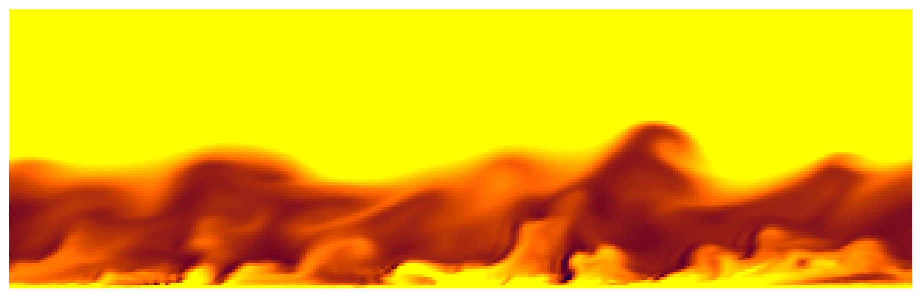

CBL with wind shear

Potential temperature field in the inversion-capped CBL (DNS visualization)

Place of CBL in the diurnal cycle of atmospheric planetary boundary layer

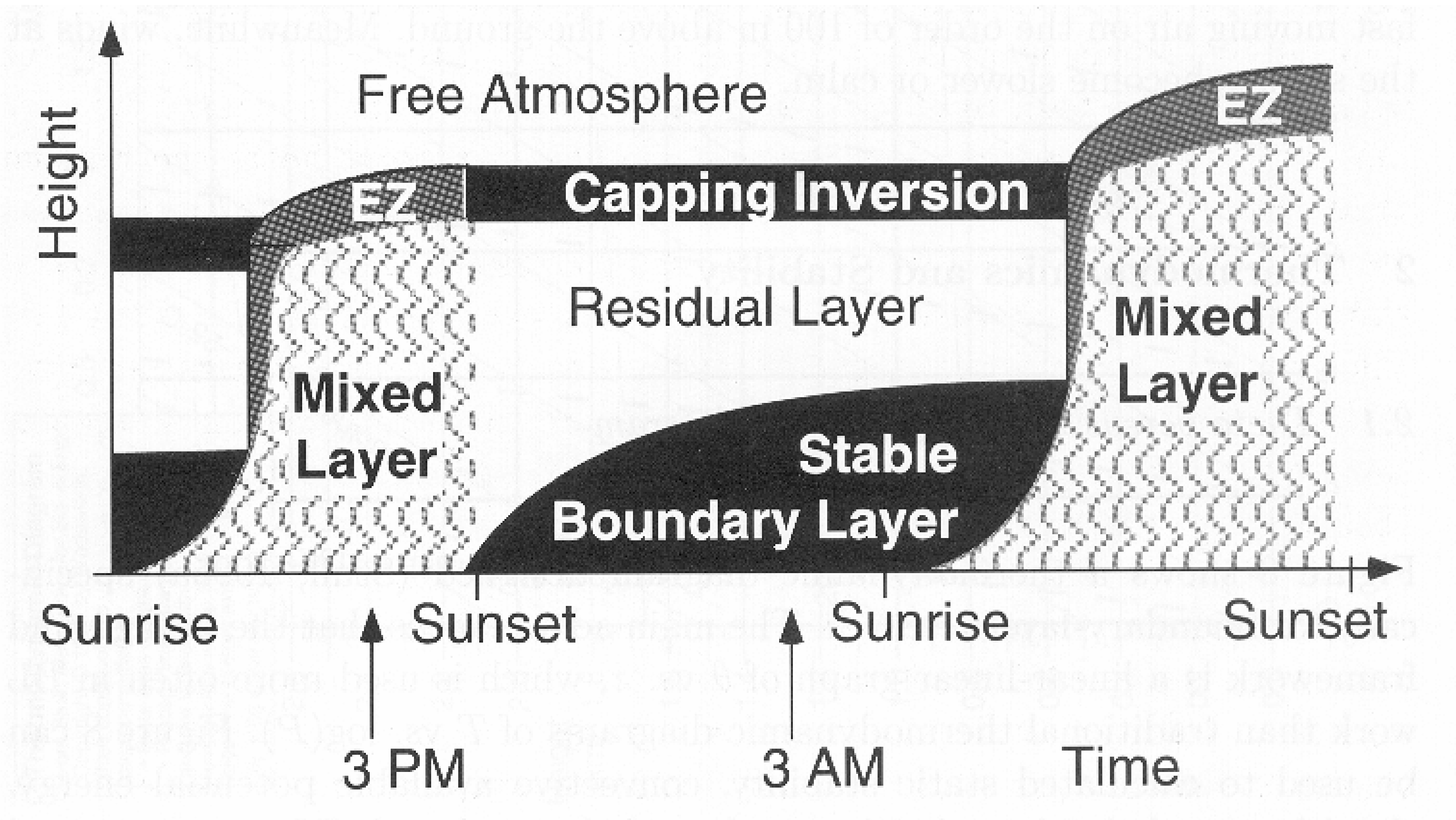

Laboratory tank modeling of CBLs

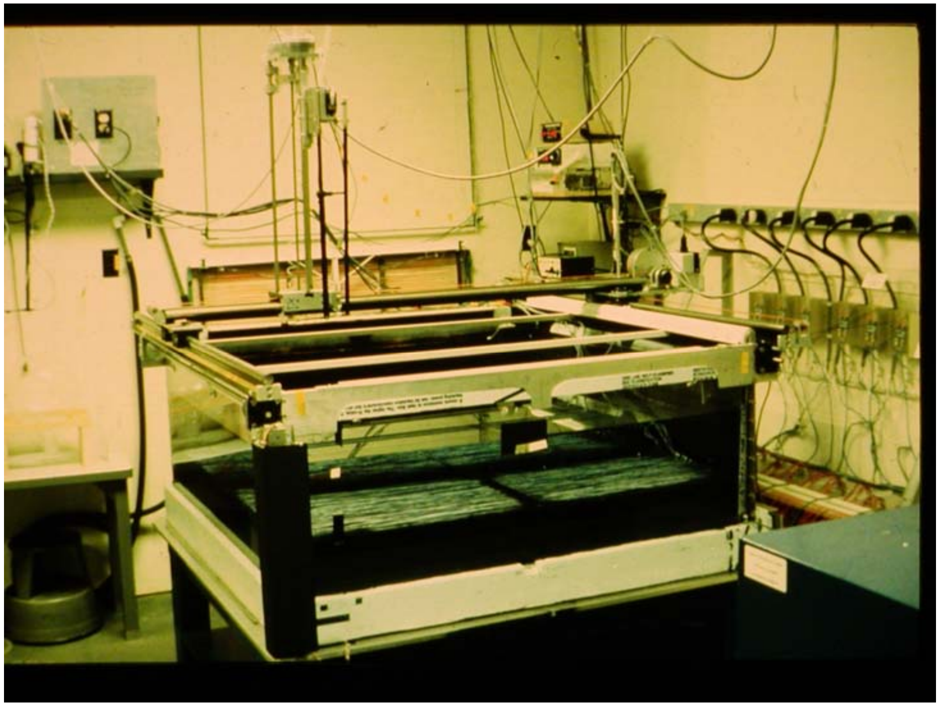

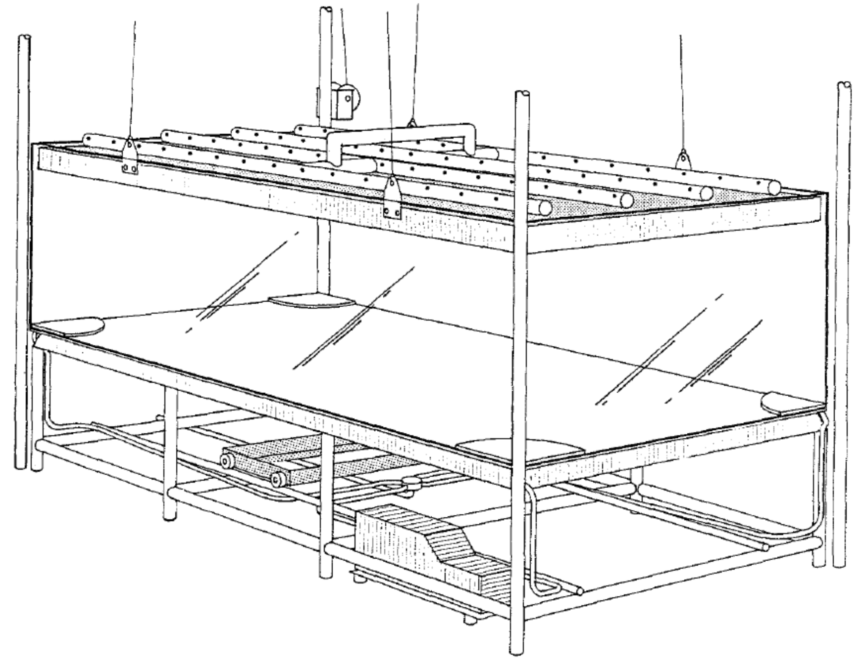

Heated water tank

Replica of Deardorff and Willis convection tank enacted in EPA (USA)

Saline water tank

"Upside-down" convection tank in use at CSIRO (Australia)

Wind tunnels to study stratified boundary layers

Colorado State University (USA)

Karlsruhe University (Germany)

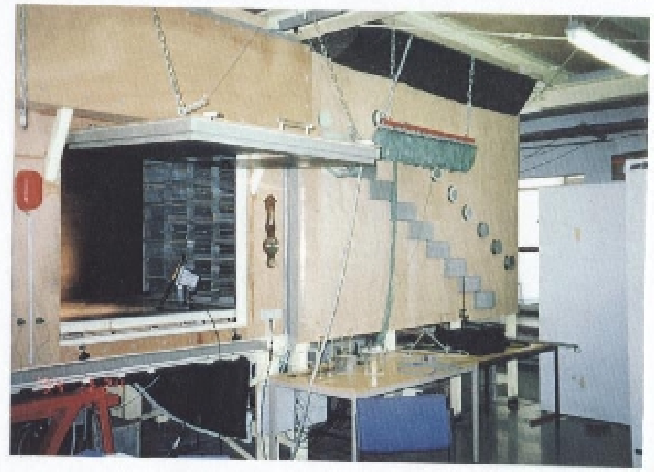

University of Surrey (UK)

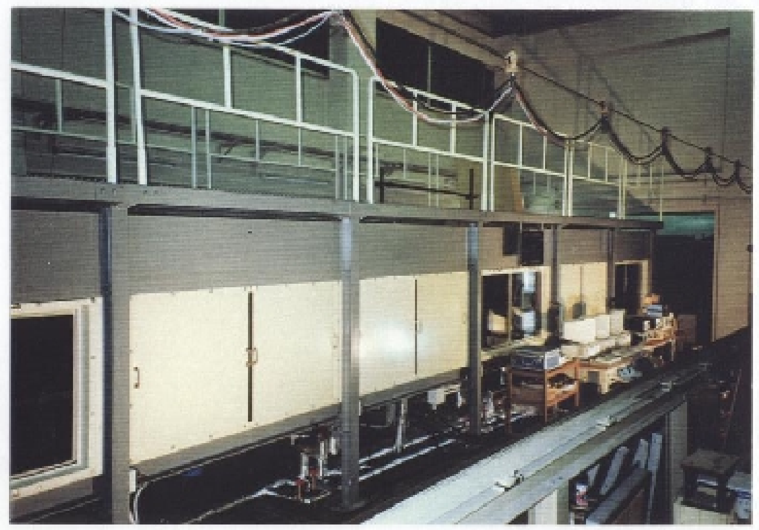

Kyushu University (Japan)

Deardorff et al. water tank model of shear-free CBL (1960-80s)

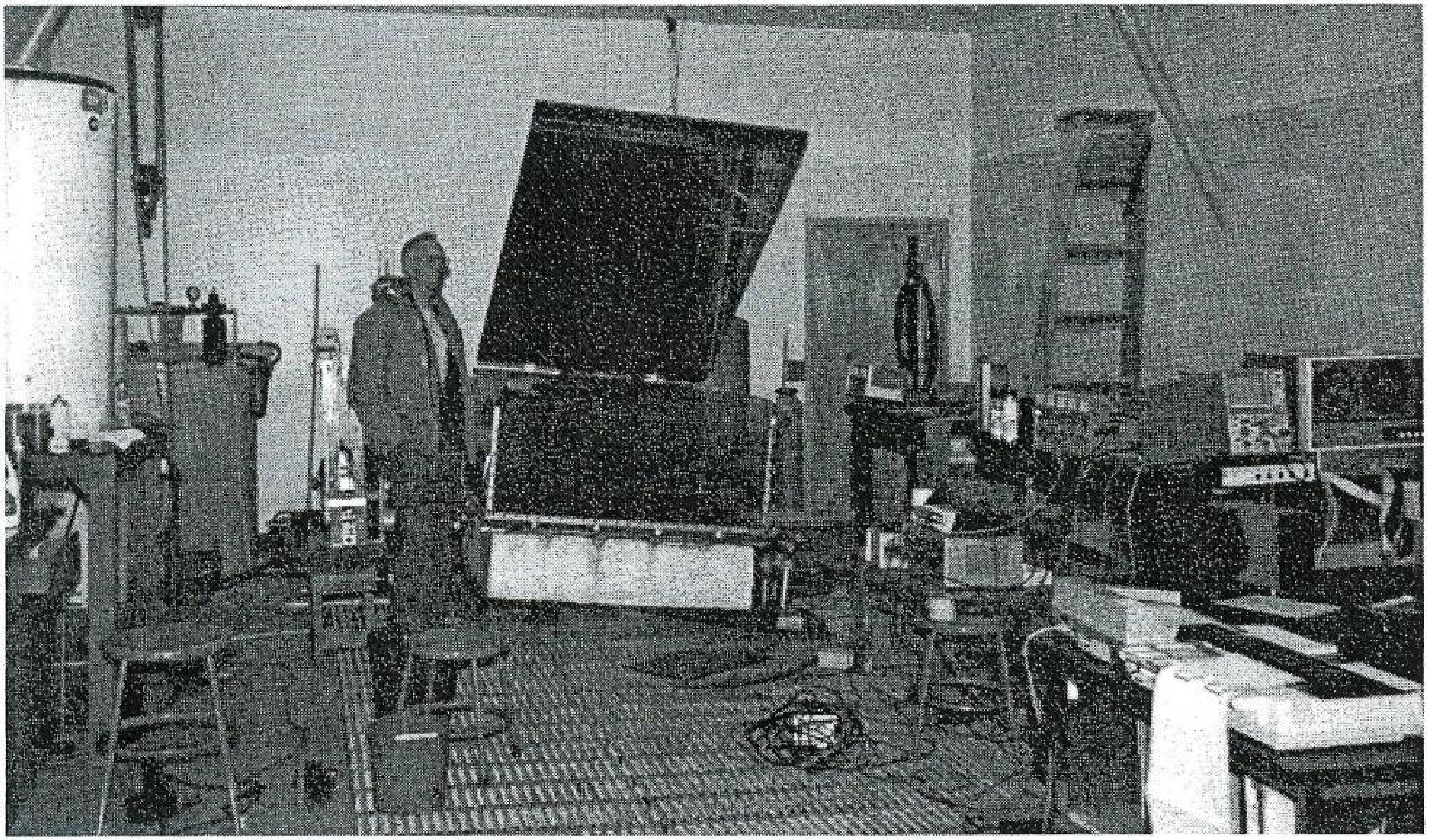

Figure 7.10 Tank used by Deardorff (pictured above) and Willis in their laboratory experiments. (Deardorff and Willis.)

From Sorbjan, Z., 1989: *Structure of the Atmospheric Boundary Layer*, Prentice Hall, 317 pp.

Willis and Deardorff convection water tank

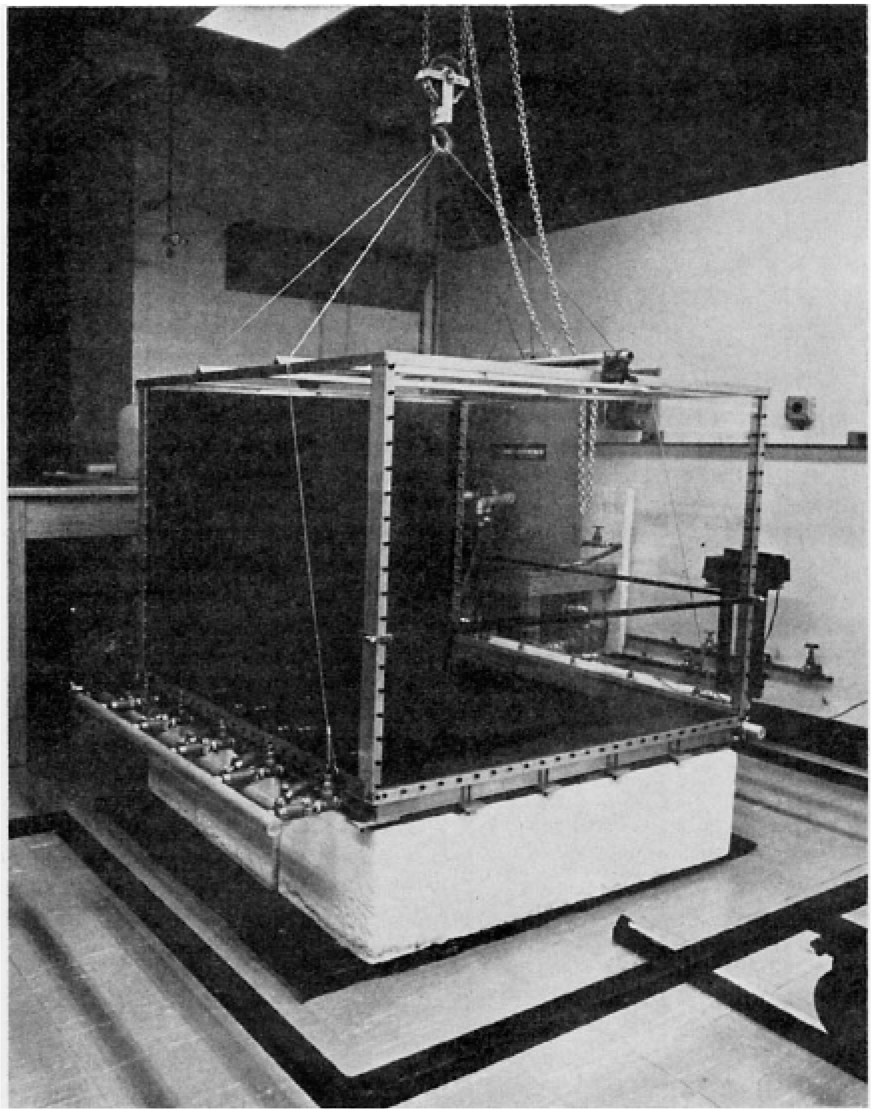

Technical data

Dimensions: 1.14×1.22×0.77 m^3

Insulation: 5-cm thick styrofoam slab at the top

Sidewalls: 1.9-cm thick plexiglass

Bottom: 1.25-cm aluminum plate

Bottom heating: circulating water heat exchanger with 10 channels at the underside of the bottom plate is used to minimize horizontal temperature gradients along the bottom of the tank

Re~4200, Re_λ~140, Ra~10^{11}

Temperature and heat flux profiles in the water tank CBL

Willis and Deardorff (*JAS*, 1974)

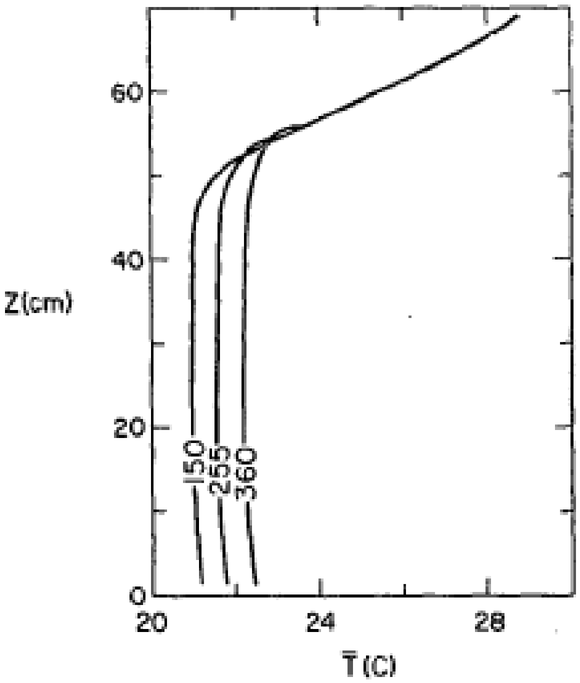

FIG. 3. Three vertical profiles of horizontally averaged temperature for stable layer case S2. Profile labels give time in seconds from beginning of experiment.

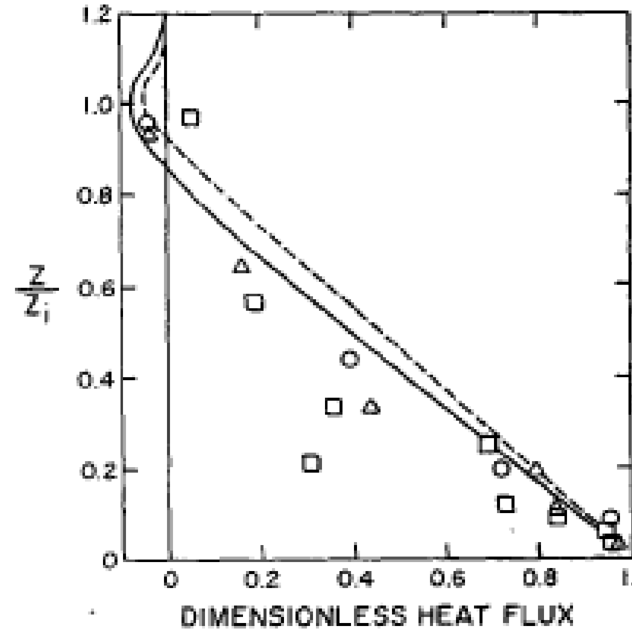

FIG. 4. Vertical profiles of dimensionless heat flux: case S1 (solid line), case S2 (dashed line). Data points are shown for (○) 25 April 1968 aircraft measurements of Lenschow (1970), (△) 13 November 1970 aircraft measurements of Lenschow (1974), and (□) aircraft measurements of Telford and Warner (1964).

Deardorff's (1970) convective scales

Velocity $w_* = (\beta Q_s z_i)^{1/3}$; **Length** z_i; **Temperature** $T_* = Q_s / w_*$,

where $\beta = g / T_r$ and Q_s is the surface kinematic heat flux

Water tank studies of convective entrainment I

Deardorff et al. (*JFM*, 1974)

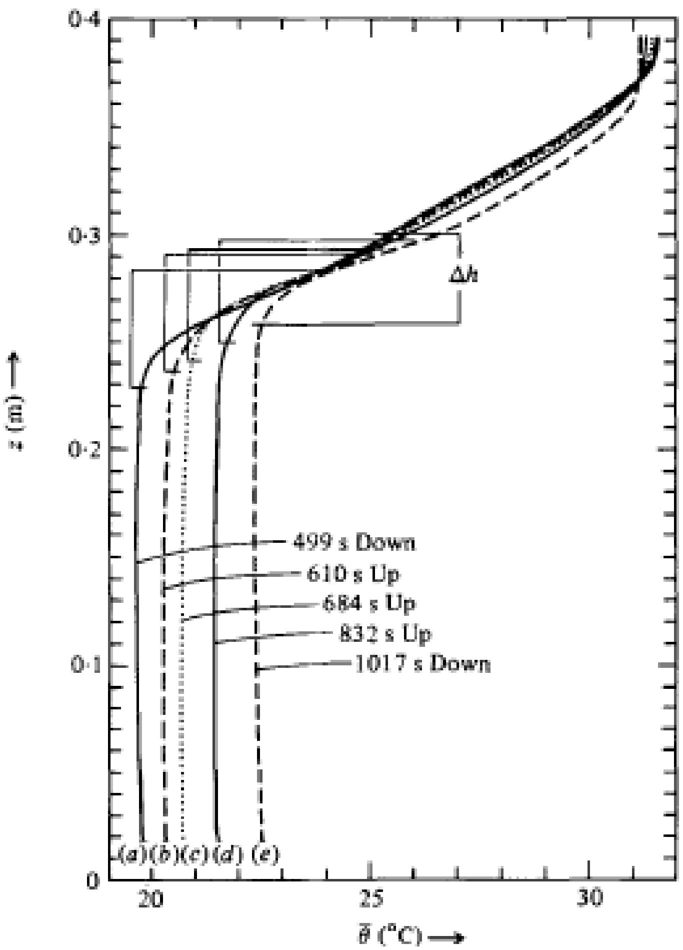

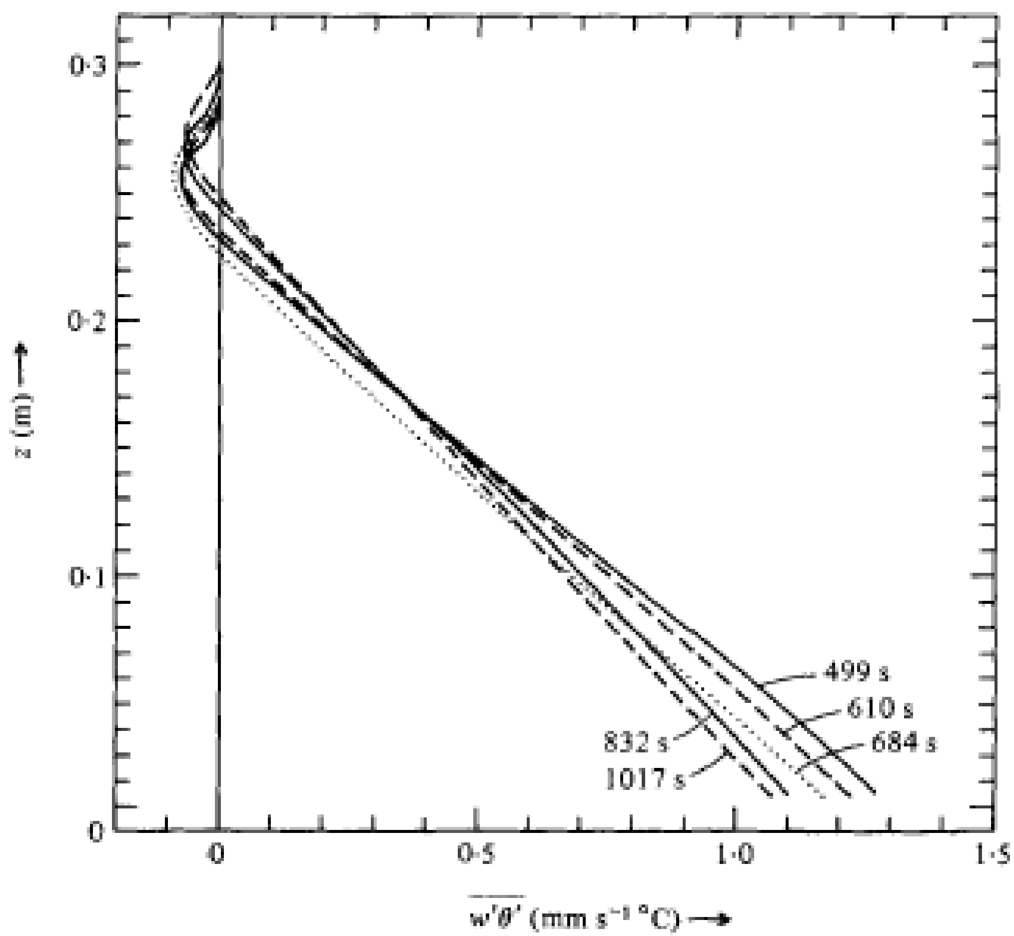

Temperature and heat flux profiles in the entraining CBL

Water tank studies of convective entrainment II

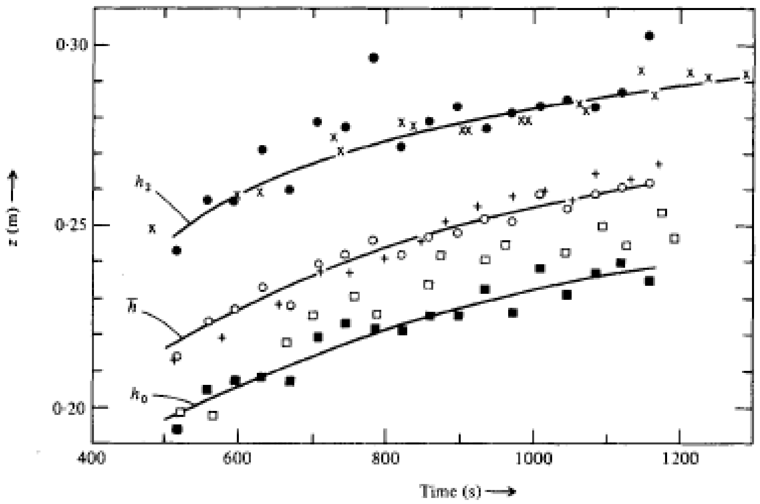

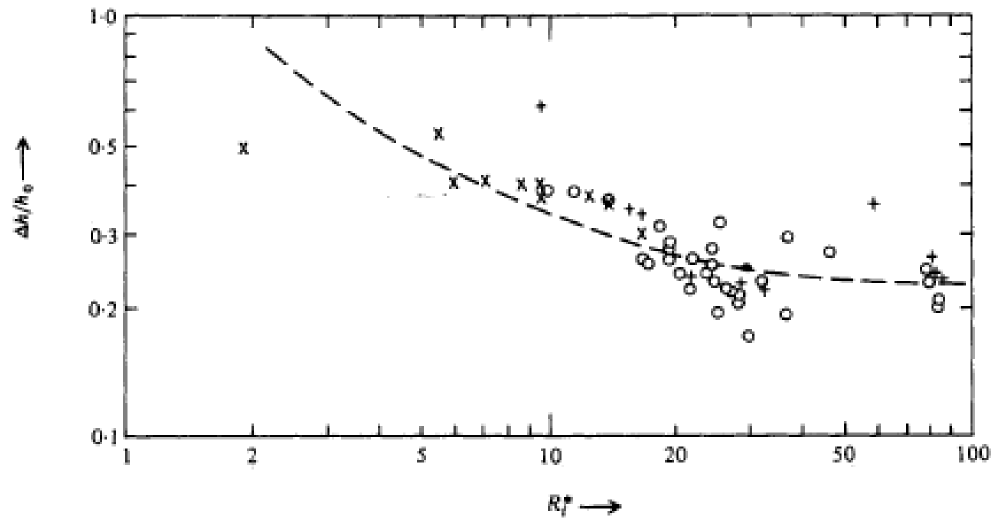

Evolution of entrainment parameters

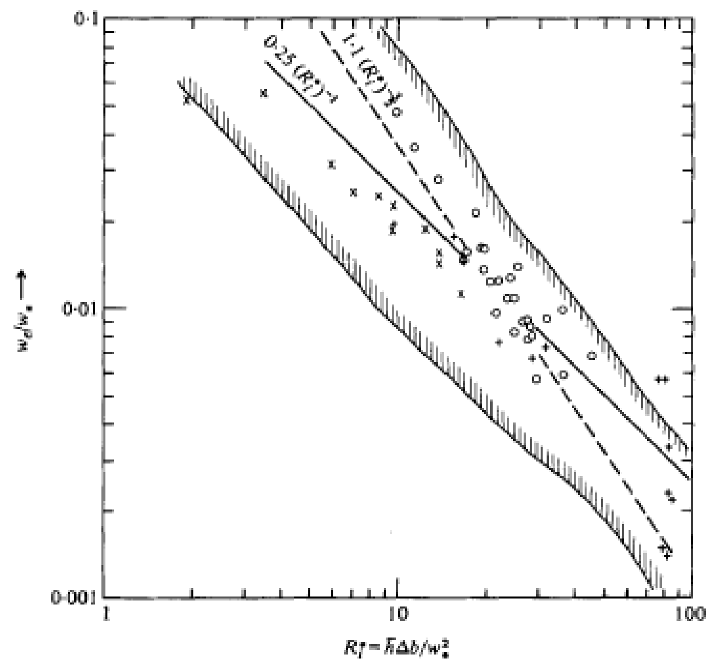

$$Ri^* = w_*^{-2} z_i \Delta b$$

$$w_e = dz_i / dt$$

$$\Delta b = \beta \Delta T$$

Water tank studies of dispersion in the CBL

Willis and Deardorff (*Atmospheric Environment*, 1978)

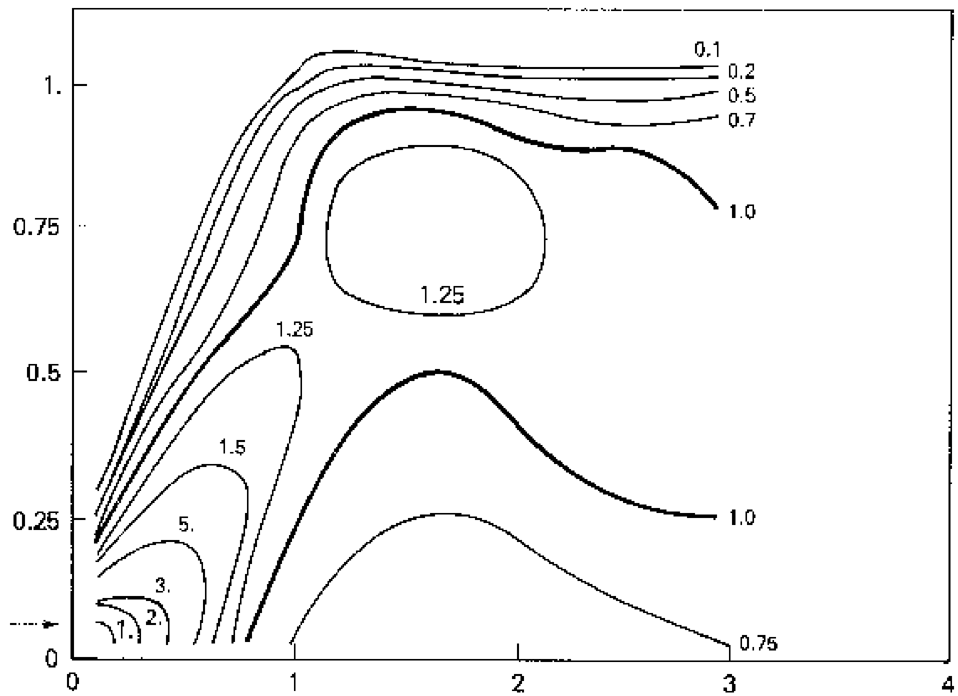

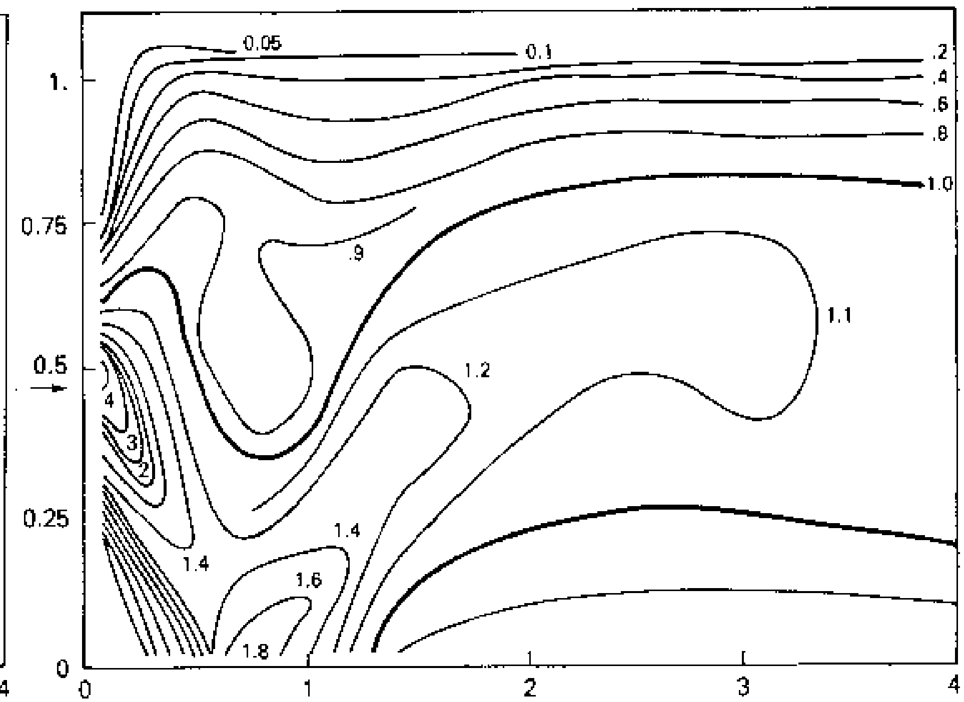

Source is at z/z_i=0.07 in the left plot and at z/z_i=0.5 in the right plot. Heights are normalized by z_i, lengths by $(z_i U)/w_*$, and concentration values by $E_s/(z_i^2 U)$, where U is the mean wind velocity and E_s [$L^3\ T^{-1}$] is the source strength. The origin of the x axis is at the source location.

Wind tunnel model of a horizontally evolving atmospheric CBL

Experimental setup in the thermally stratified wind tunnel of UniKA

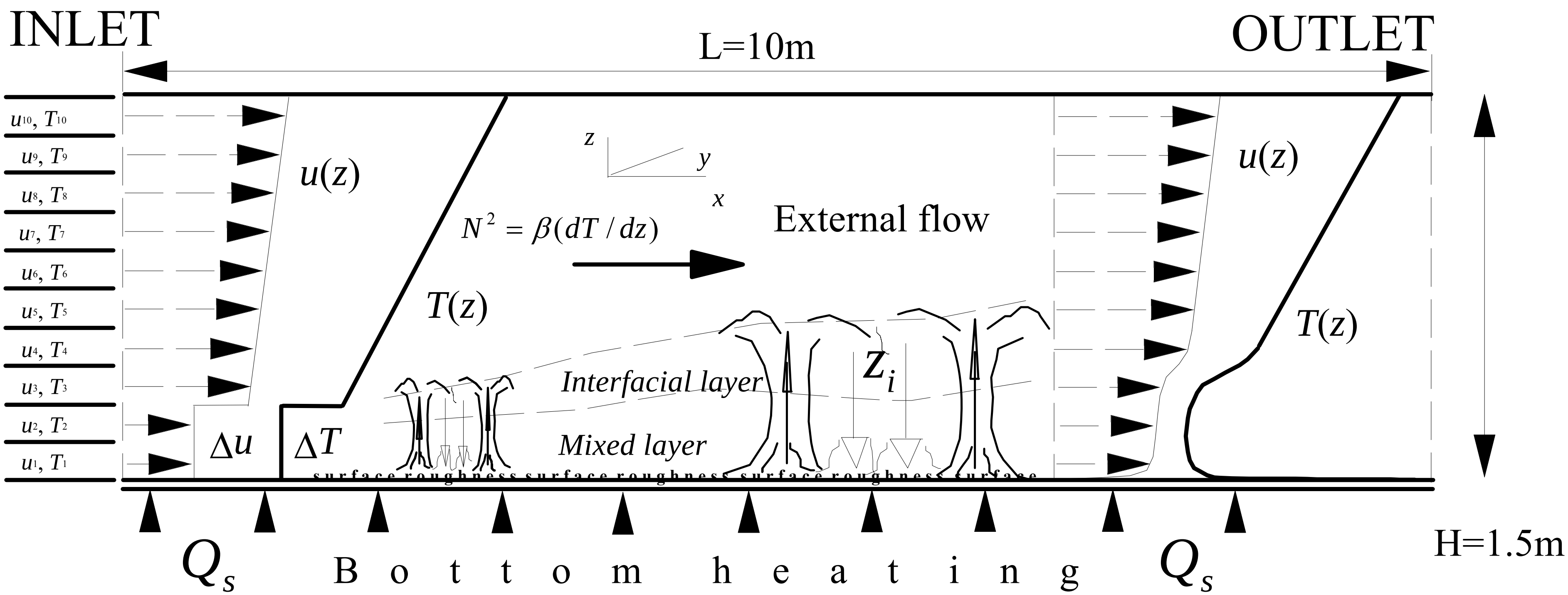

Richardson numbers: $\mathrm{Ri}_{\Delta T} = \beta w_*^{-2} z_i \Delta T$ and $\mathrm{Ri}_N = N^2 z_i^2 w_*^{-2}$

Shear/buoyancy forcing ratio: u_* / w_*, where $w_* = (\beta Q_s z_i)^{1/3}$

Atmospheric CBL:	$\mathrm{Ri}_{\Delta T}$<100	Ri_N<100	u_* / w_*<1
UniKA wind tunnel:	$\mathrm{Ri}_{\Delta T}$<10	Ri_N<20	$u_* / w_* \approx 0.3$
Water tank, D-W:	$\mathrm{Ri}_{\Delta T}$=15	Ri_N=100	u_* / w_*=0 **(shear-free CBL)**

UniKa thermally stratified wind tunnel

Interior of the tunnel

Exterior of the tunnel

Visualized CBL flow

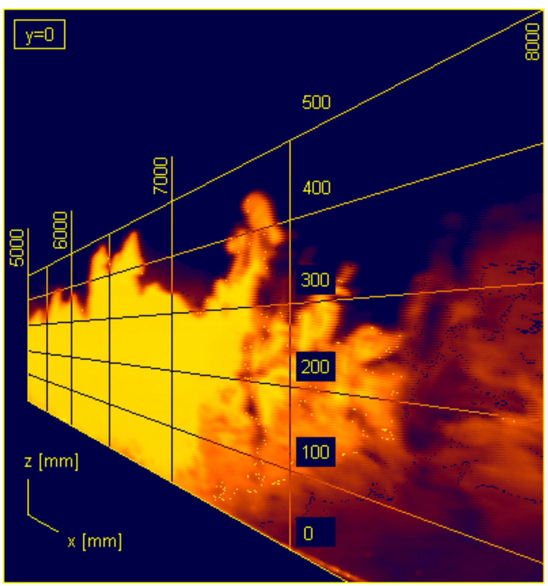

Visualized neutral BL flow

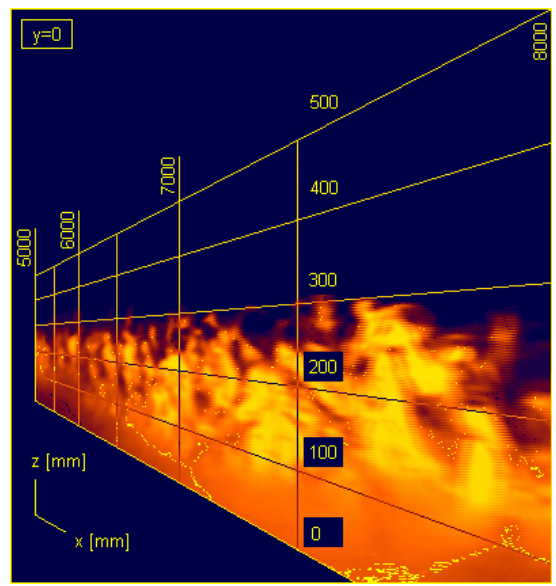

Flow evolution in the UniKa wind tunnel model of CBL

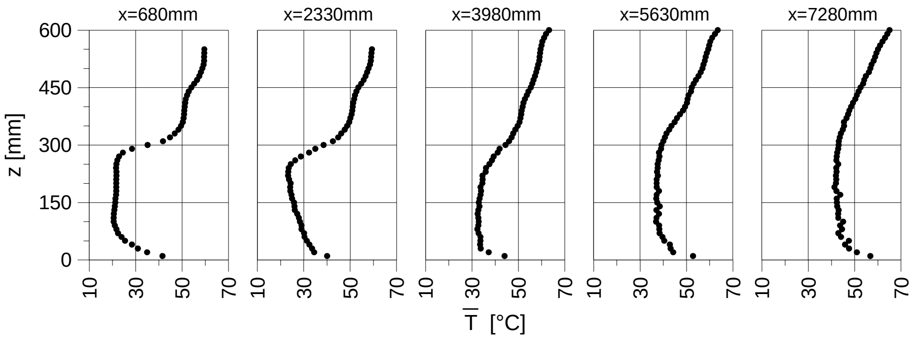

Mean temperature

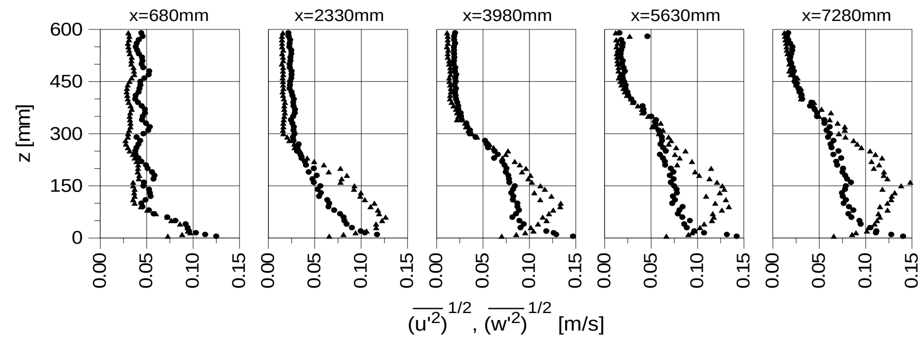

Velocity fluctuations

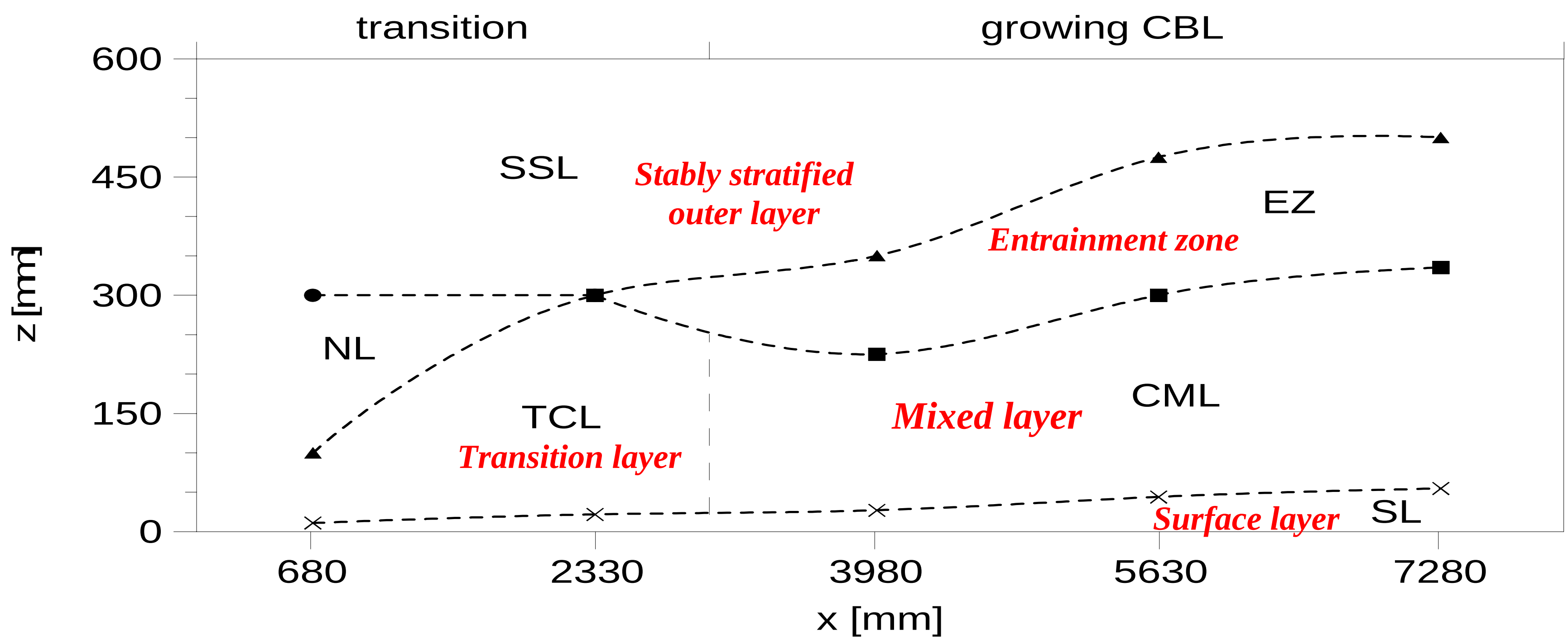

Sublayers within the modeled CBL and flow evolution stages

Large eddy simulation of horizontally evolving CBL

Parameter	Setting
Domain size	$10\times1.5\times1.5 m^3$ (UniKA WT test section)
Grid	$400\times60\times60$
Surface kinematic temperature flux	$1 K\cdot m\cdot s^{-1}$
Temperature stratification above CBL	$33 K\cdot m^{-1}$
Time advancement	Leapfrog scheme with a weak filter
Outflow boundary conditions	Radiation conditions for prognostic variables + mass-flux outflow correction
Lateral and top boundary conditions	No-slip + log wall law for velocity; zero-gradient for other prognostic variables
Inflow boundary conditions	Preset stationary fields of mean velocity and temperature with superimposed non-correlated random fluctuations of prescribed r.m.s. magnitude
Bottom boundary conditions	No-slip for velocity; zero-gradient for other prognostic variables; Monin-Obukhov similarity functions implemented locally to relate surface fluxes and gradients
Subgrid turbulence closure	Subgrid TKE-based (Deardorff 1980)

Visual comparison of simulated and modeled (WT) flows

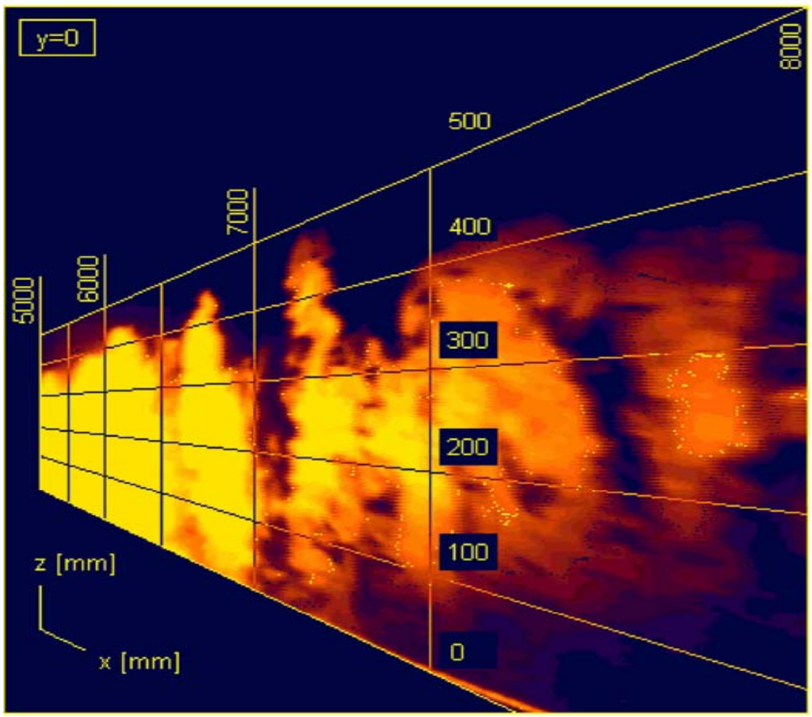

Visualization in the wind tunnel

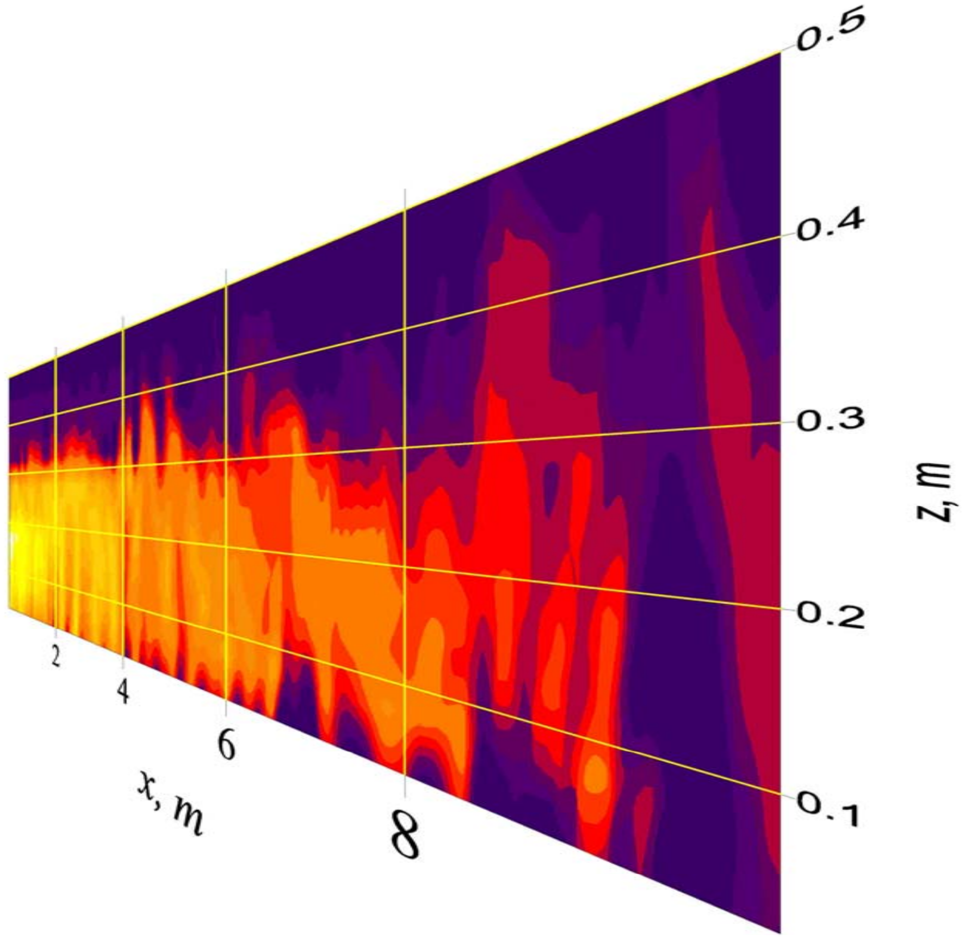

Temperature pattern from LES

Changes of flow structure across the inversion layer

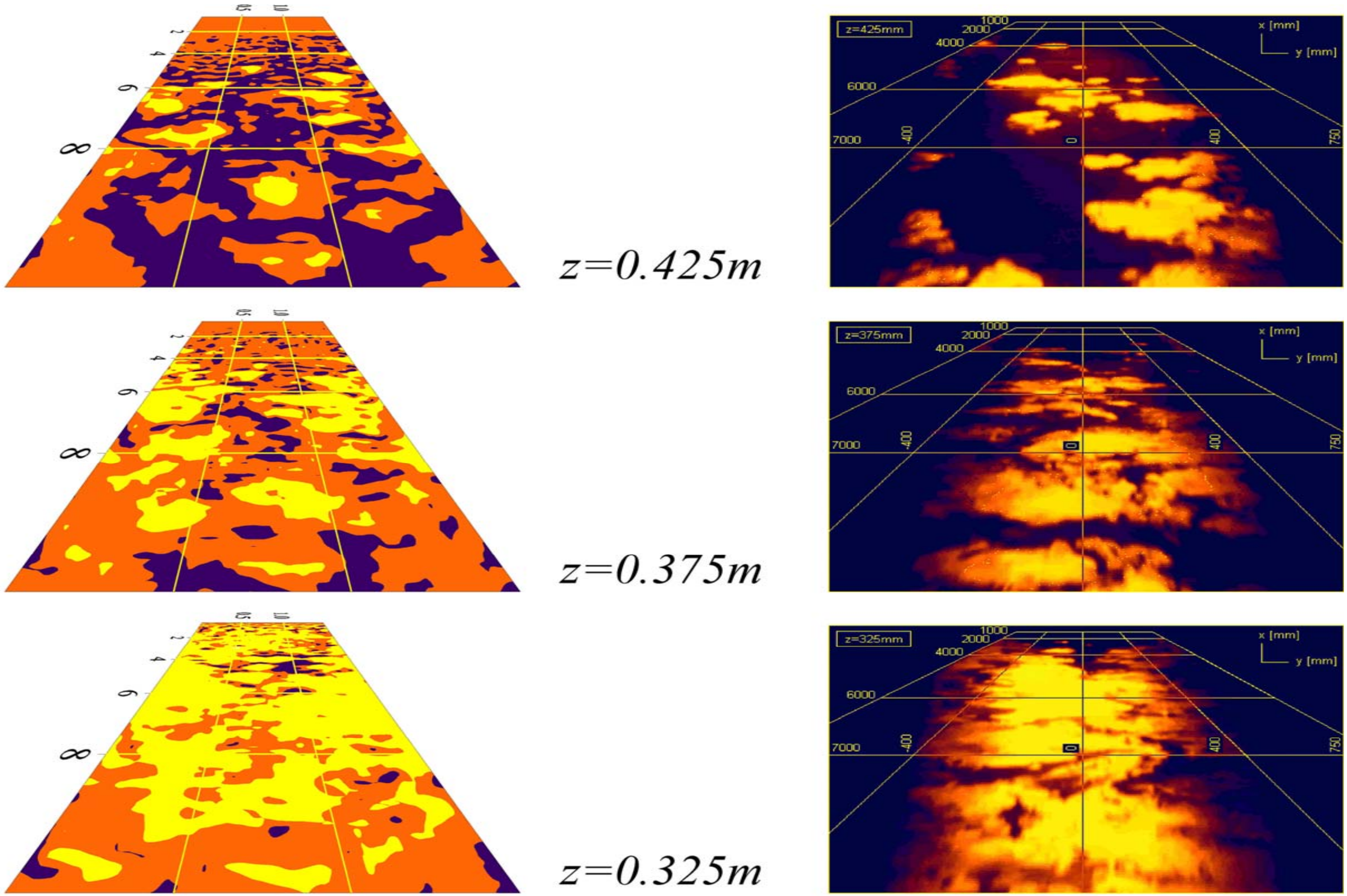

Temperature pattern from LES

Visualization in the wind tunnel

Evolution of flow fields in the wind tunnel CBL: LES data

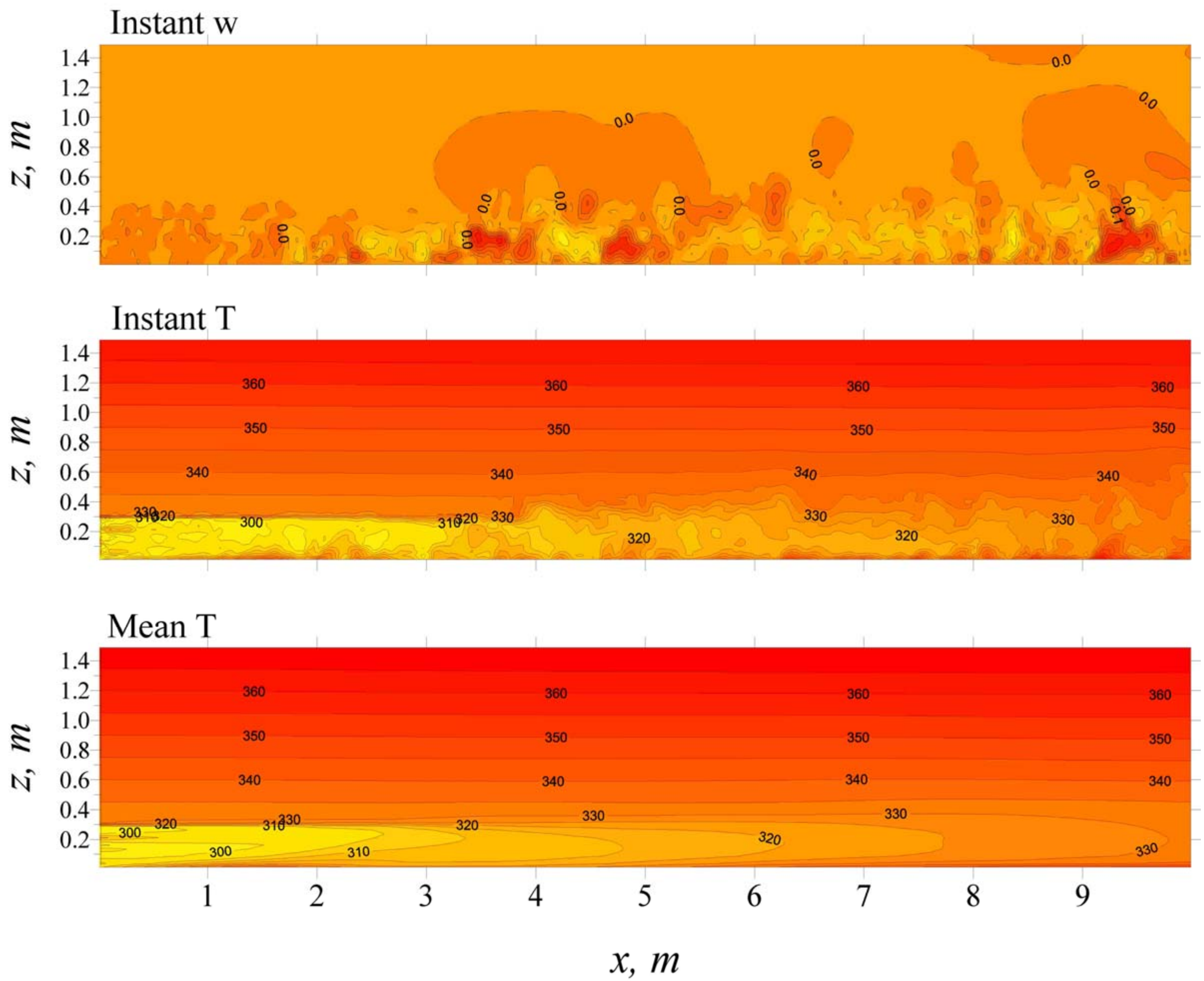

Role of inflow conditions in transition to well-mixed CBL

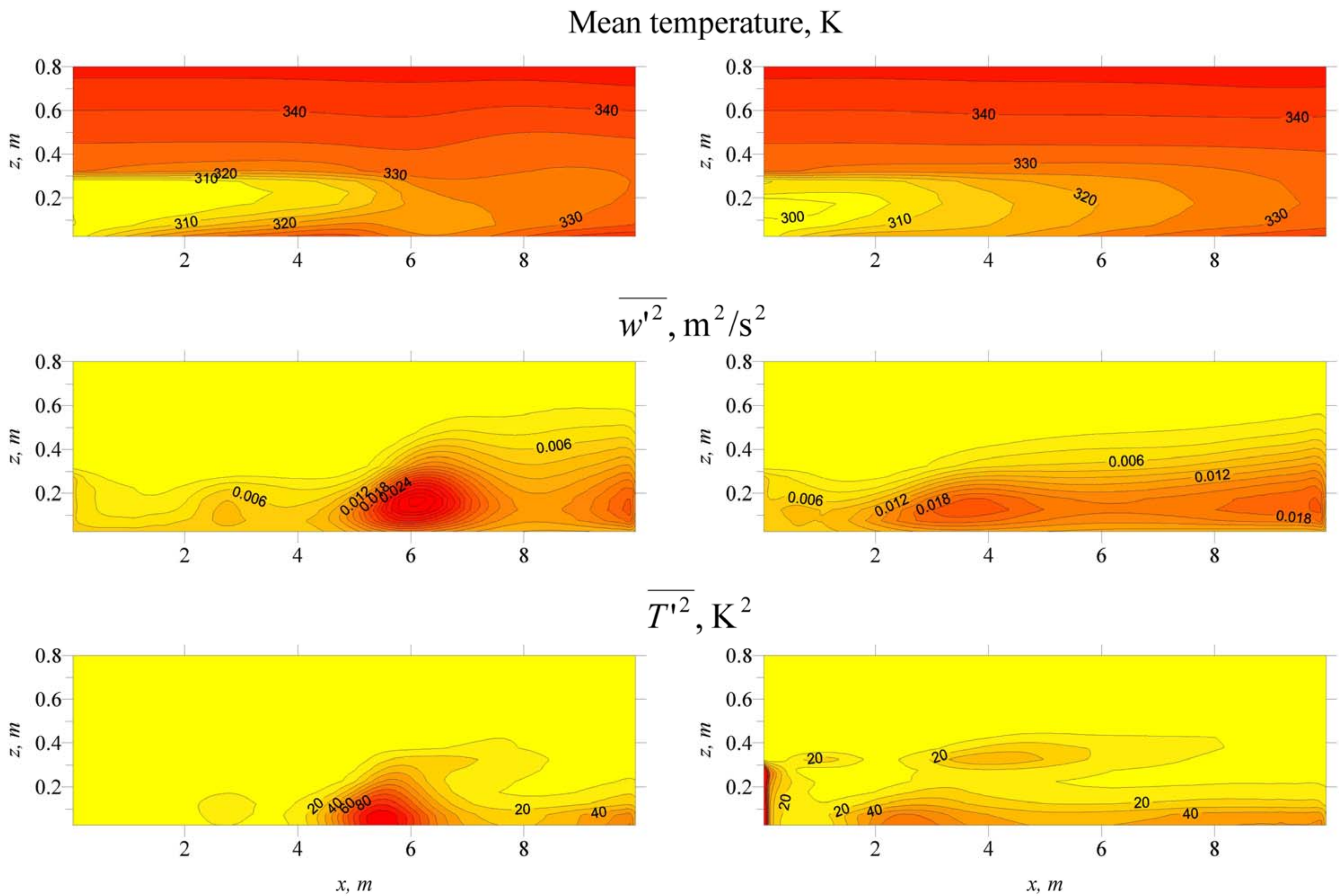

Inflow without disturbances

Inflow temperature agitated below the inversion

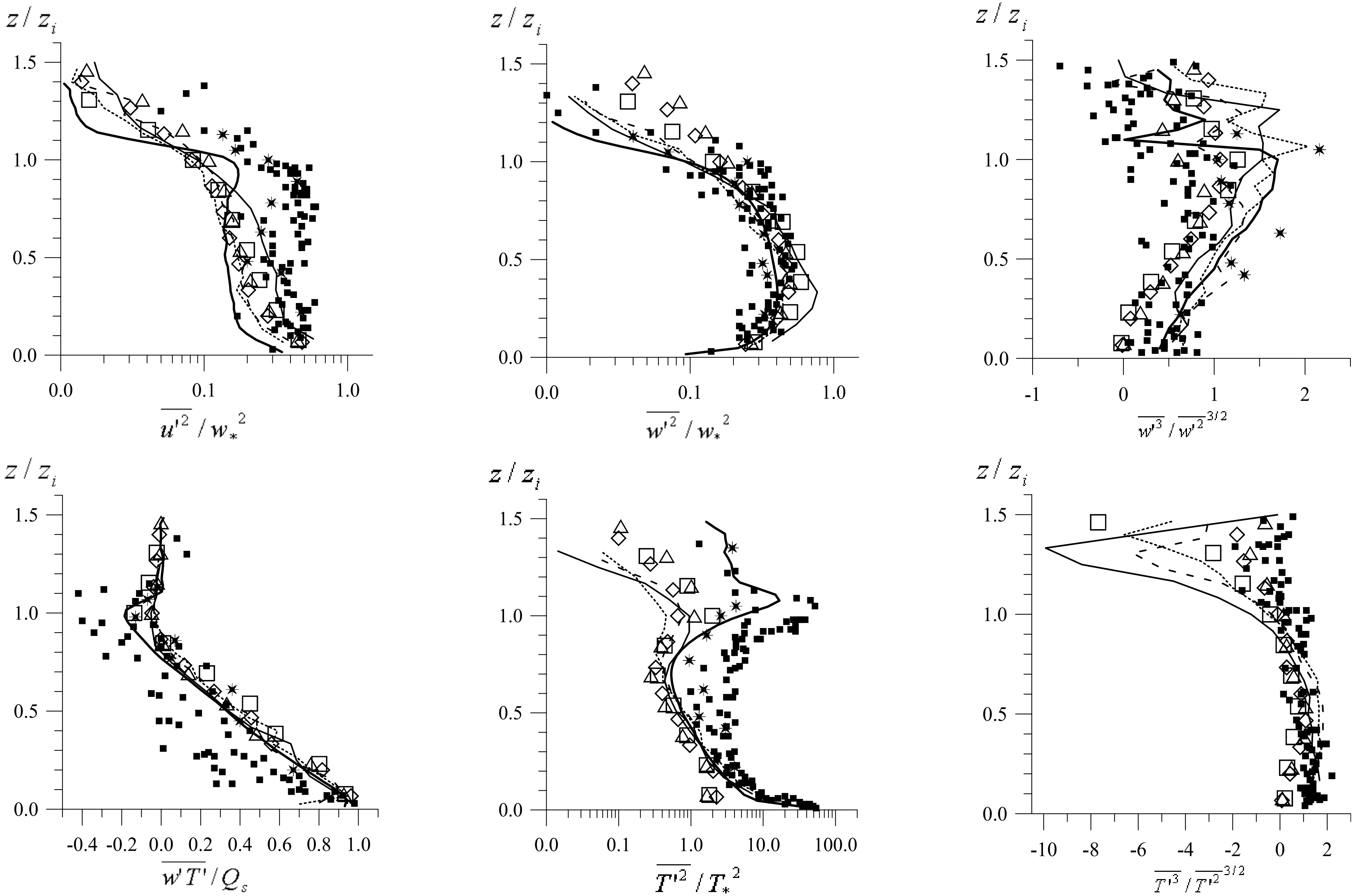

Thin lines: WT (3 windows); **B**old lines: LES (shear-free CBL); **O**pen symbols: LES of WT CBL (3 windows); **F**illed squares: atmosphere; **A**sterisks: water tank.

Joint probability density of *T′* and *w′* in the WT CBL

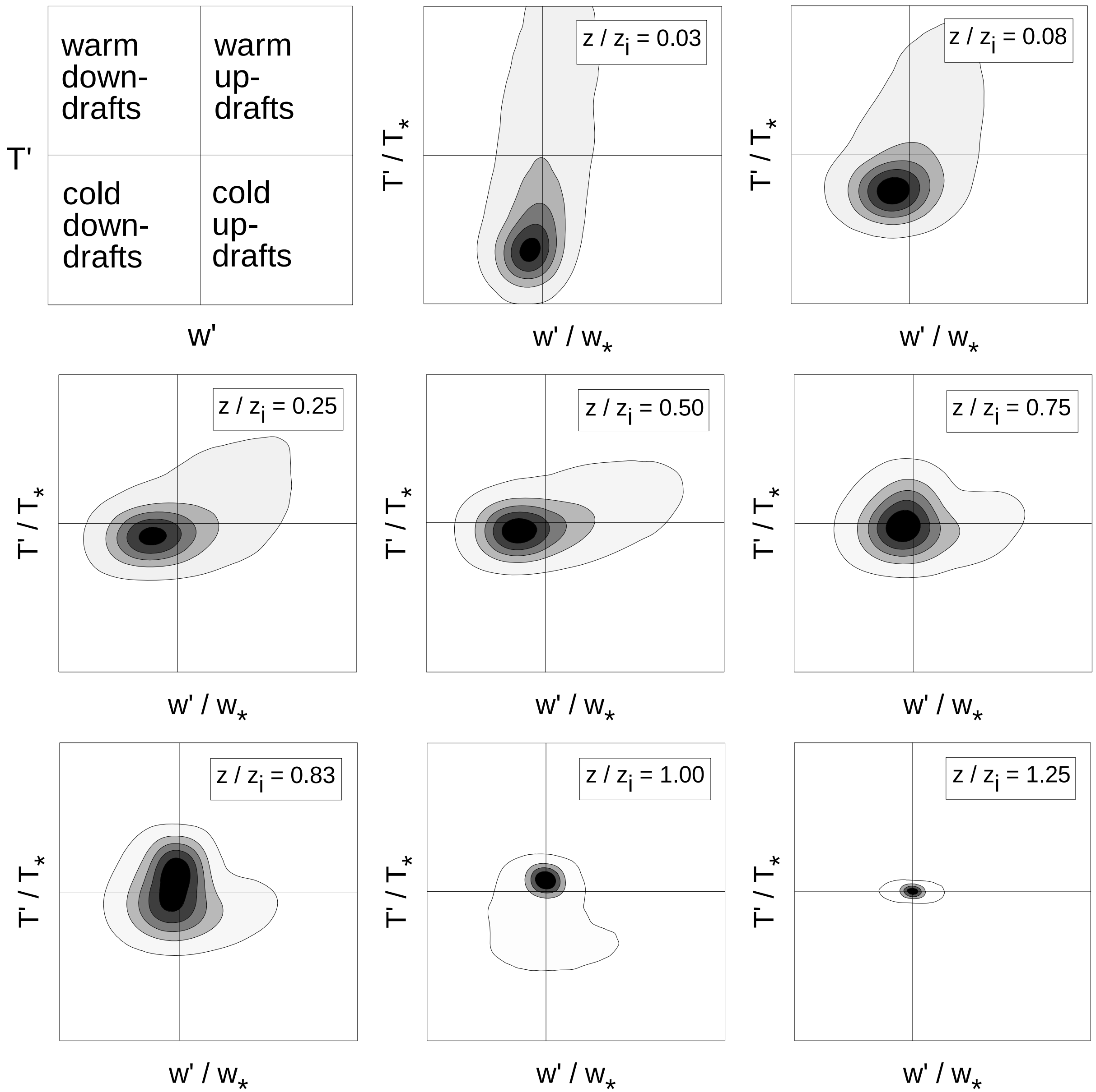

Density distributions of T' and w' at x=3.98 m

Velocity and temperature spectra in the wind tunnel CBL

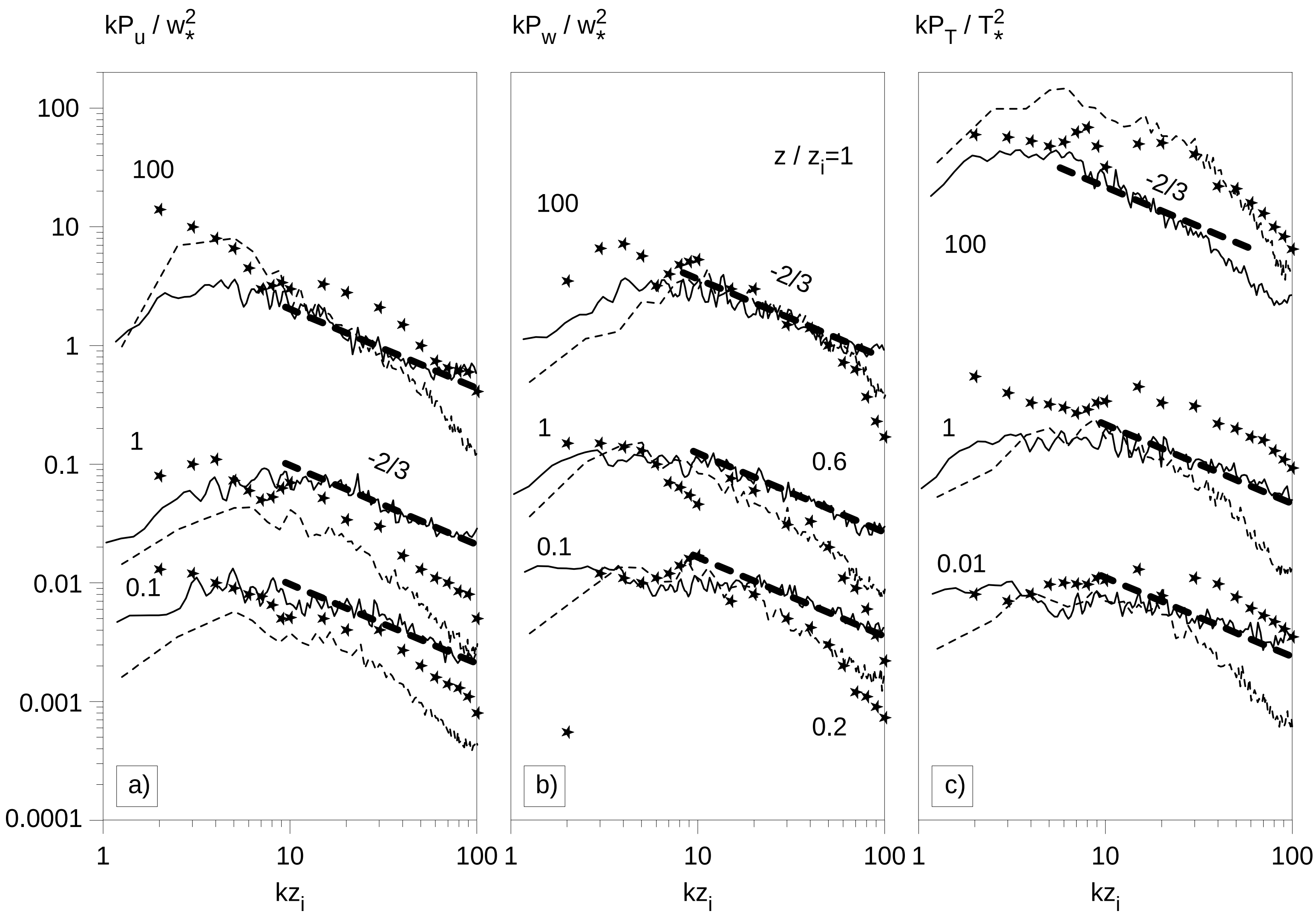

Solid lines: spectra of (**a**) longitudinal velocity, (**b**) vertical velocity, and (**c**) temperature in the wind tunnel CBL. Stars: water tank spectra of Deardorff and Willis (1985). Dashed lines: LES of shear-free CBL of Schmidt and Schumann (1989)

Turbulence anisotropy and dissipation rates in the WT CBL

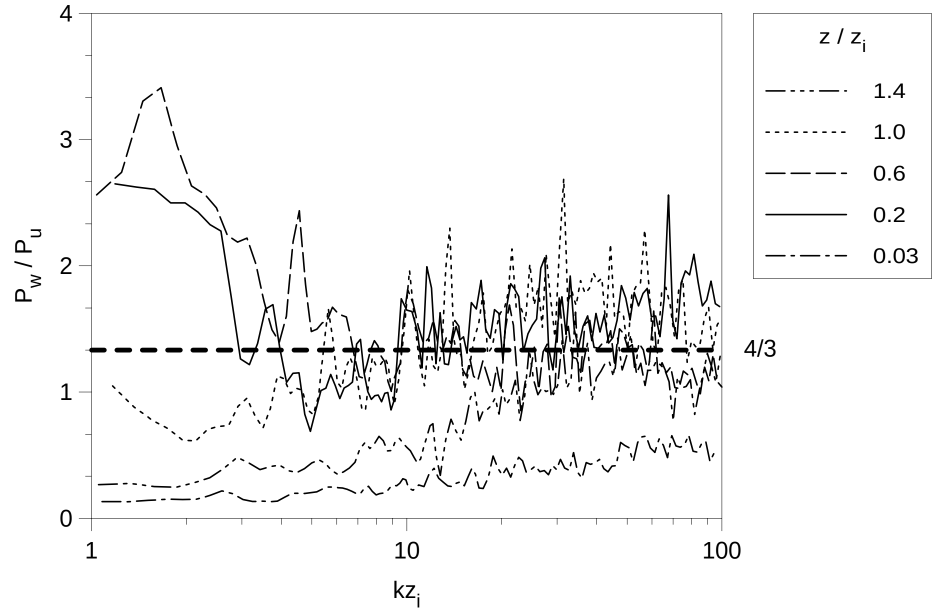

Spectral ratio P_w / P_u at different dimensionless elevations

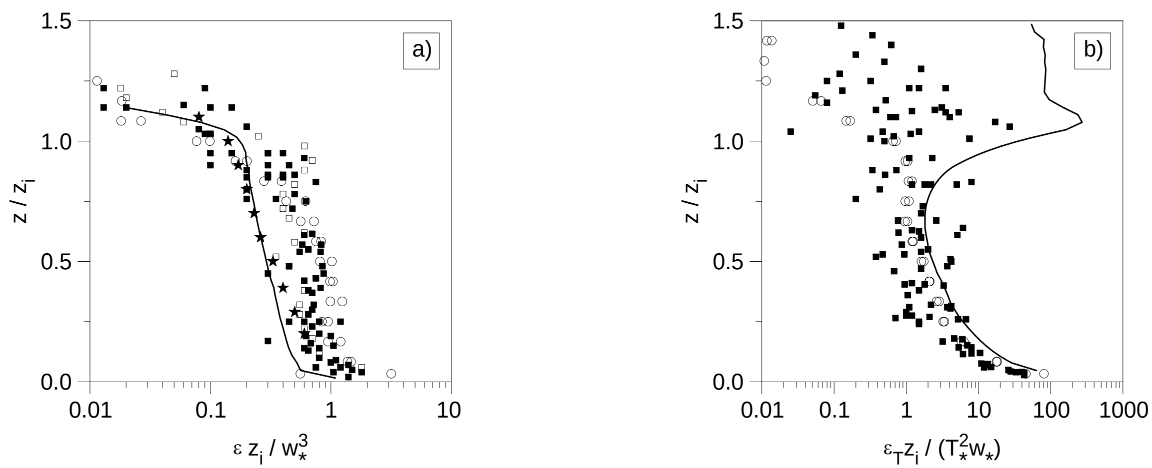

TKE dissipation rate (a), and temperature fluctuation destruction rate (b). Tunnel: circles. Atmosphere: filled squares. Tank: stars. Ocean: empty squares. LES of shear-free CBL: lines

Effect of elevated shear on the CBL deepening (WT data)

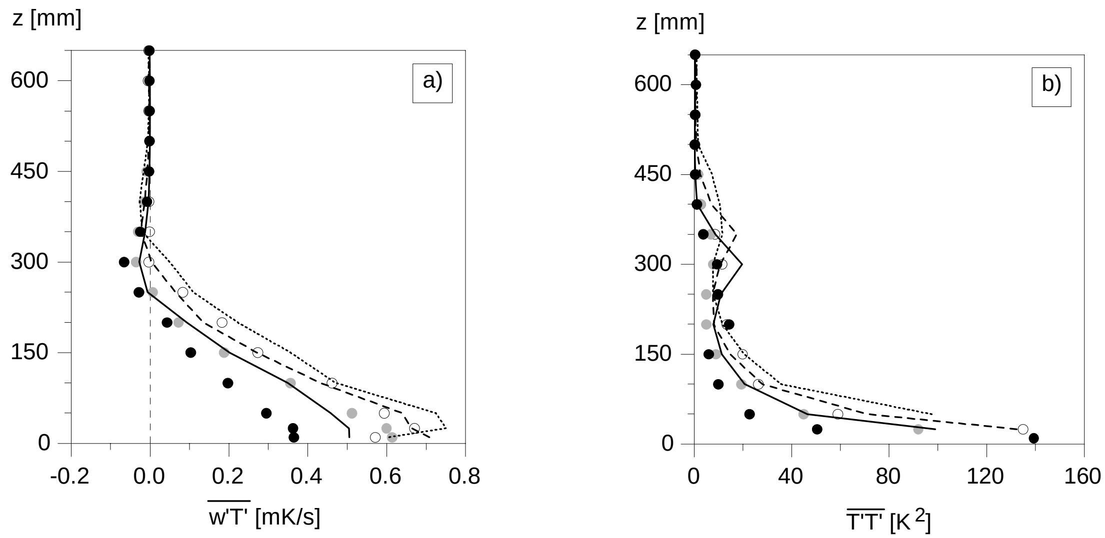

Without elevated shear: lines. In the presence of positive elevated shear: points.

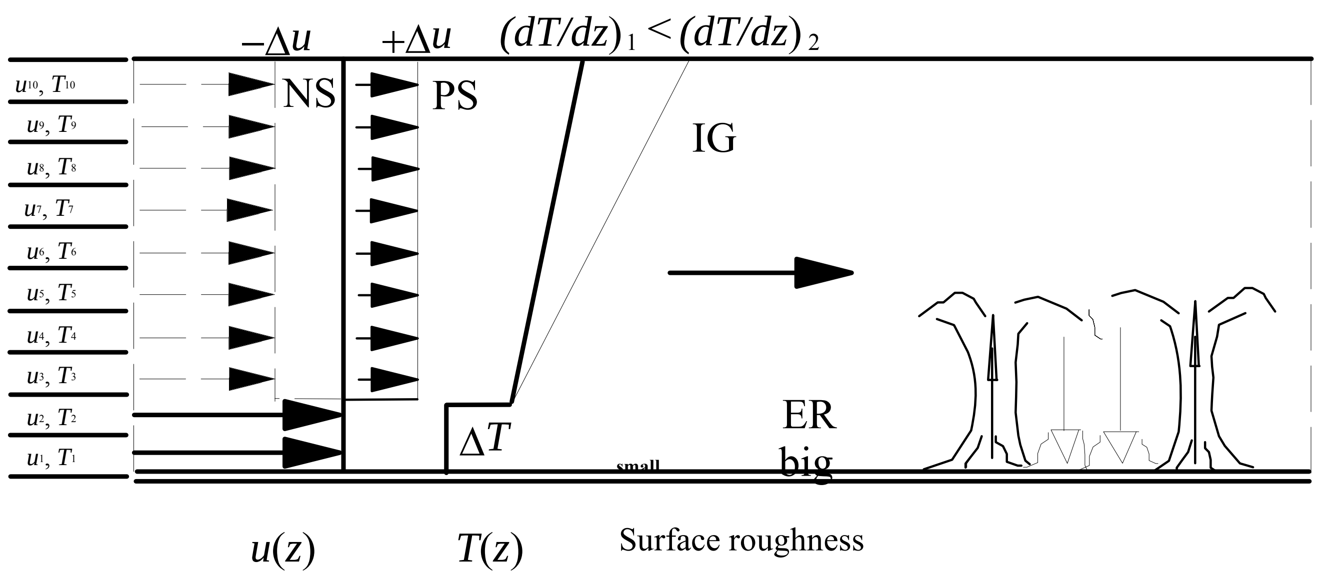

Using LES to study a variety of CBL flow regimes

Shear versus entrainment in control of the CBL growth

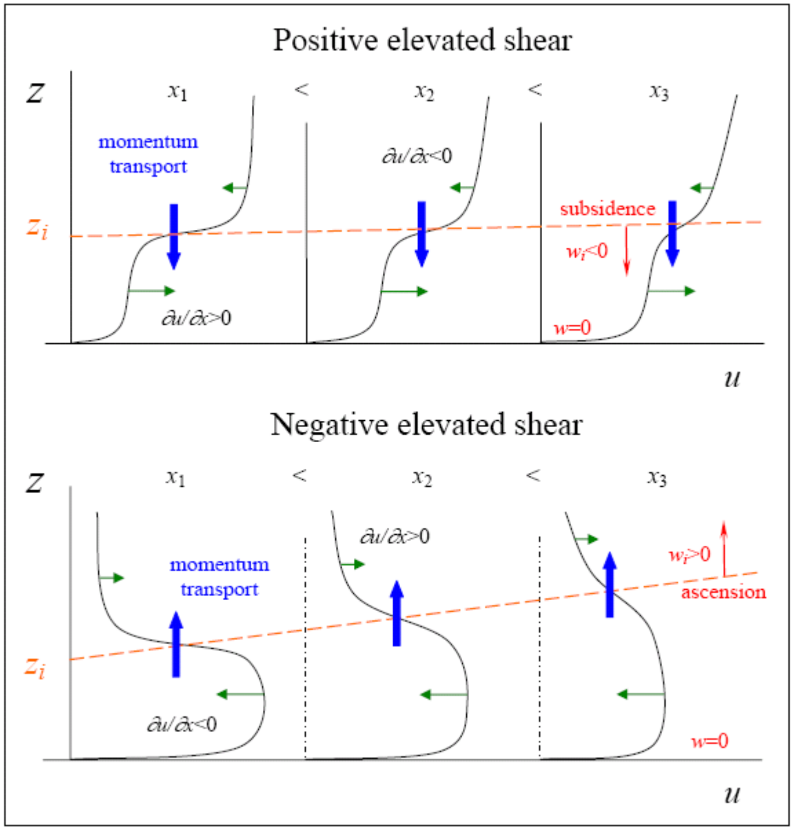

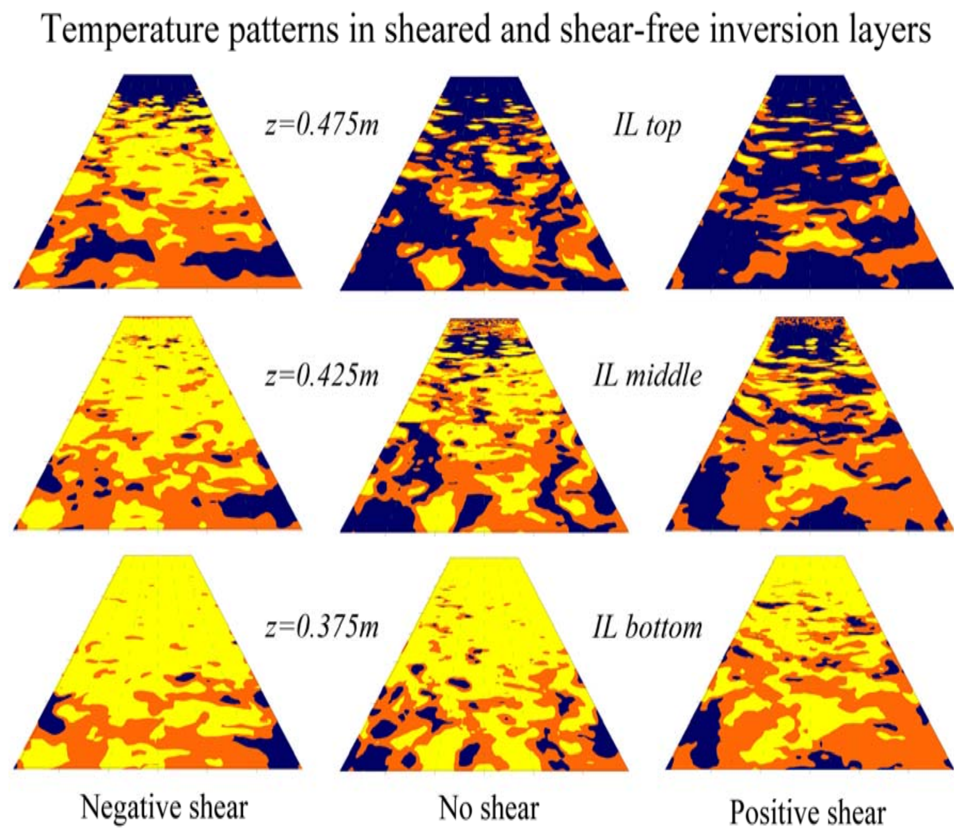

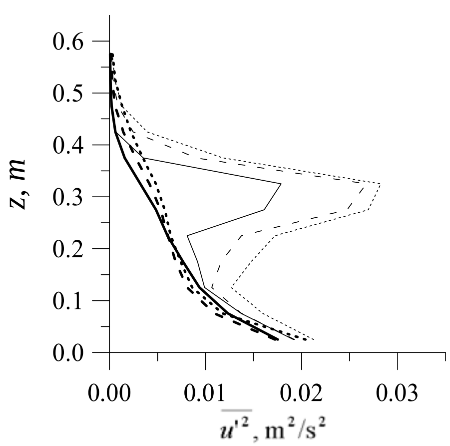

Positive shear

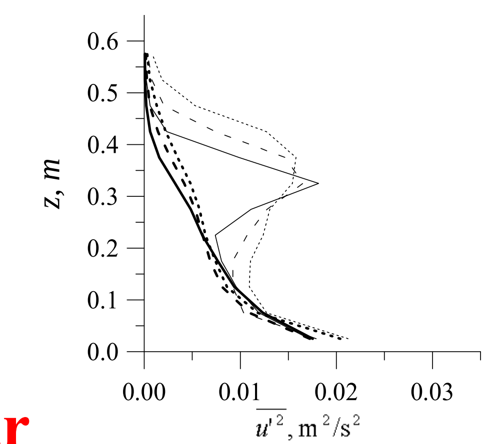

Negative shear

Combining WT modeling and LES to study dispersion in the CBL

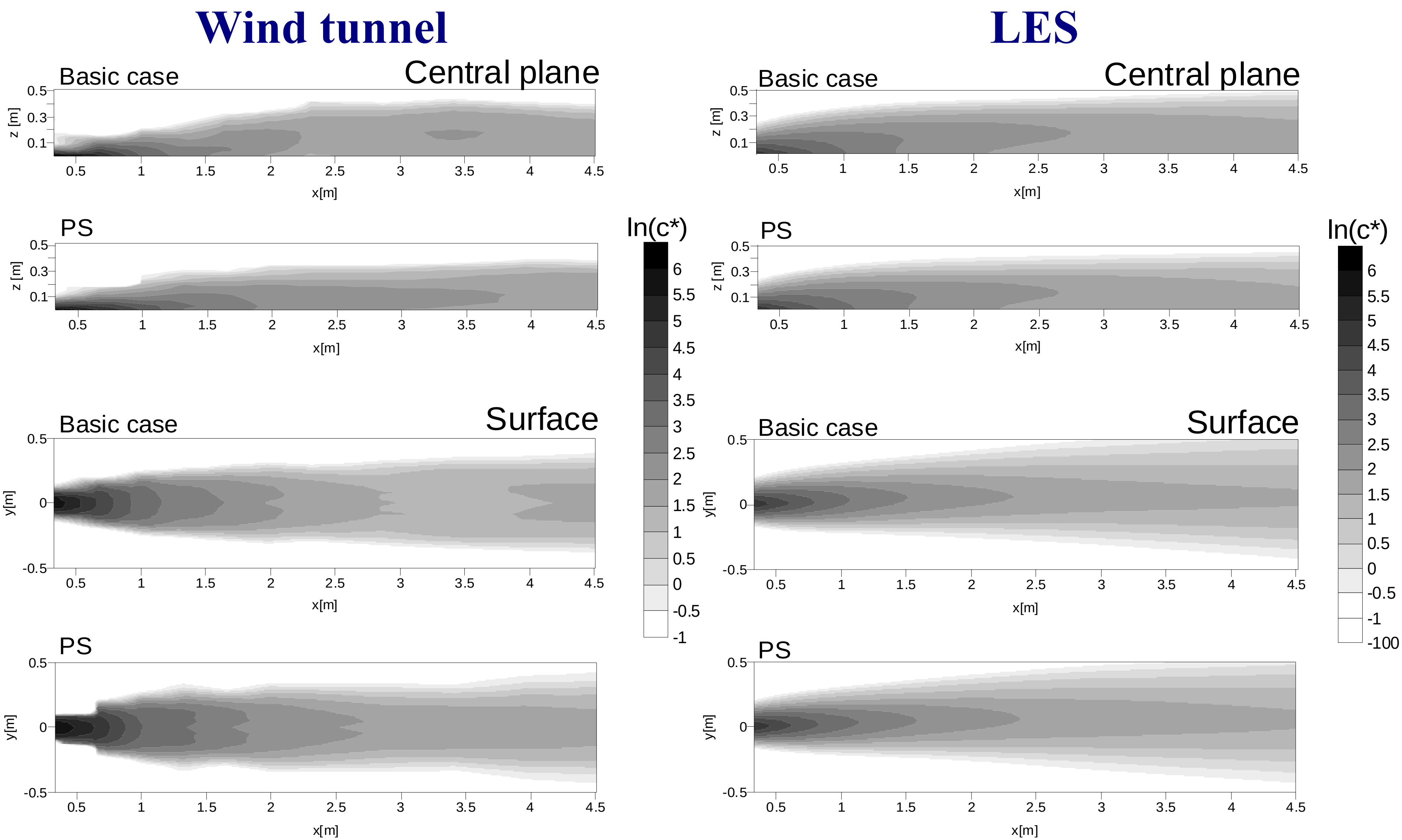

Point source is at the ground level. The origin of the *x* ordinate is at the source location. The capping-inversion and shear-zone elevation at *x*=0 is 0.3 m.

Comparison with water tank data of Willis and Deardorff

Water tank

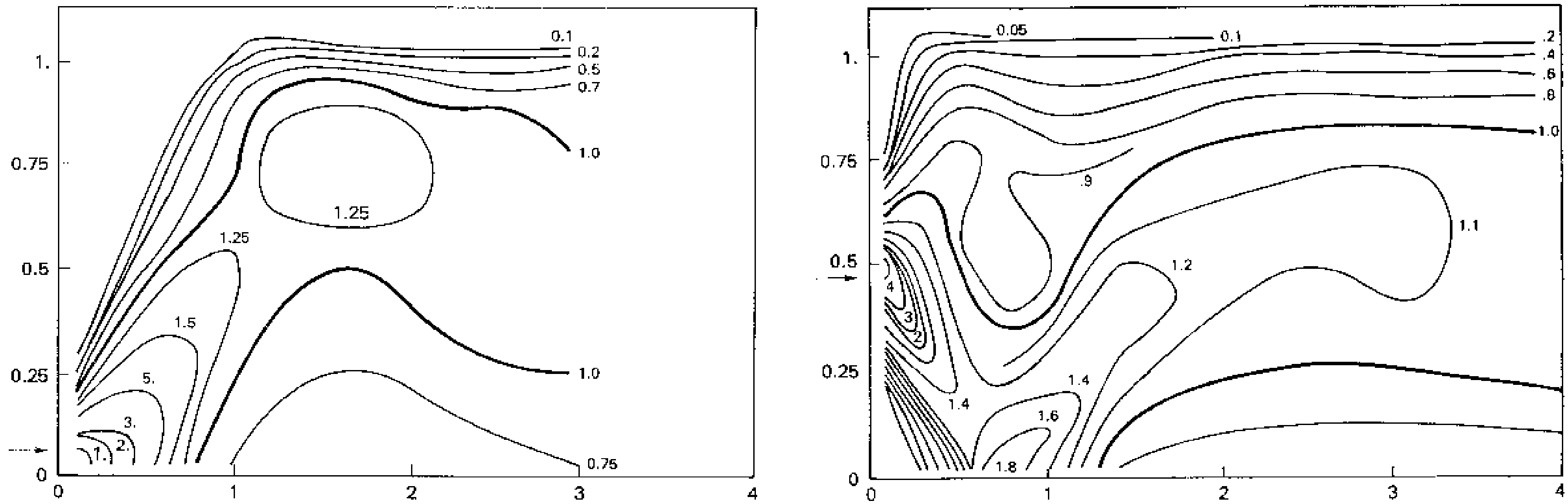

Wind tunnel

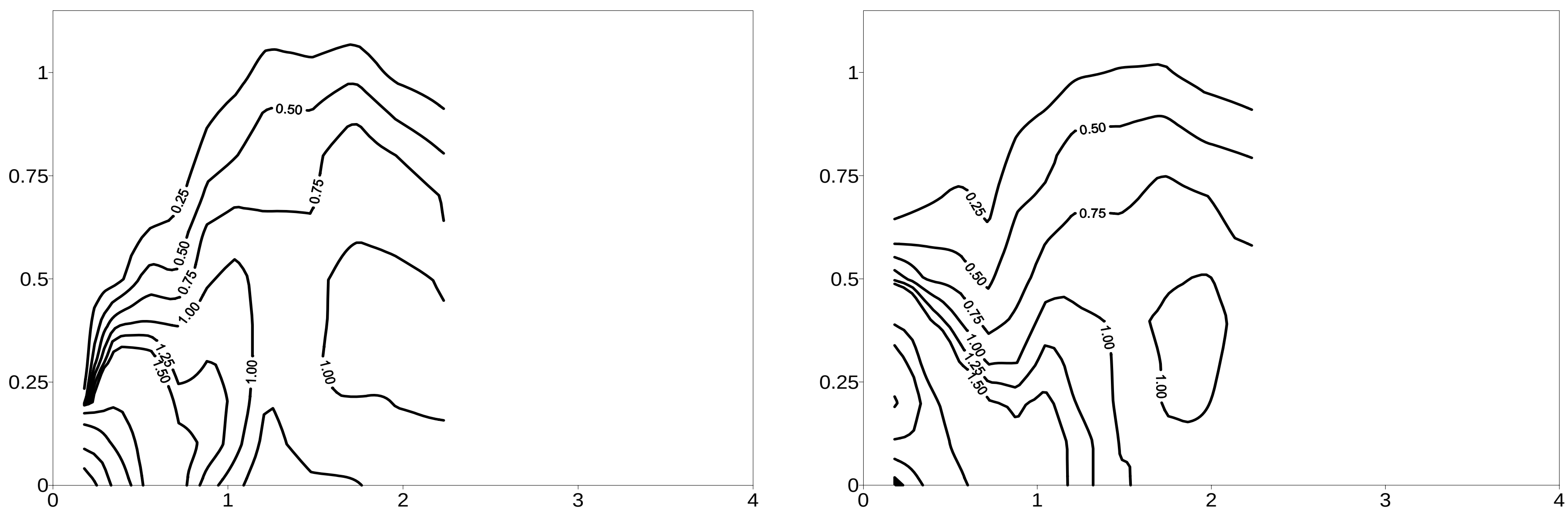

Using WT and LES output to feed Lagrangian dispersion model

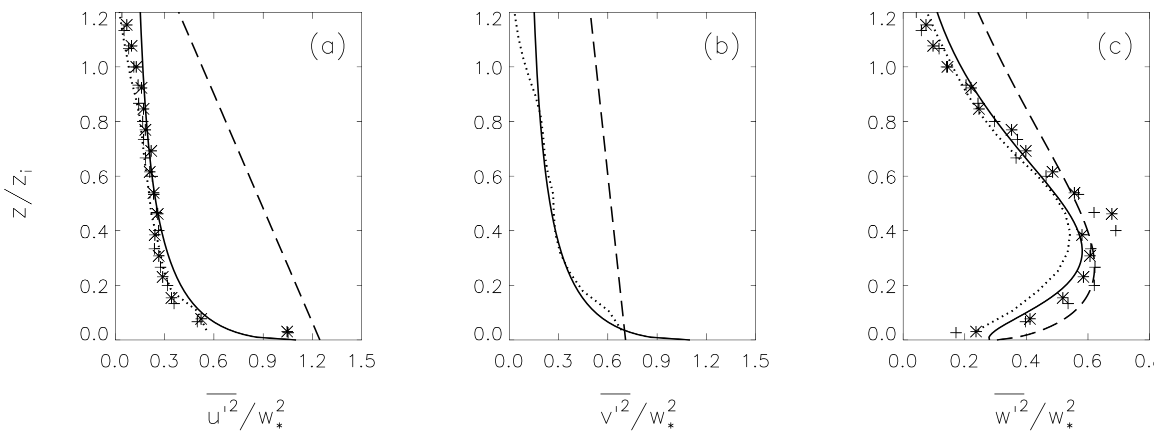

Original (dashed lines) and new (solid lines) **turbulence parameterizations** in the Rotach et al. (1996) Lagrangian dispersion model.

Markers are WT data, dotted lines are LES data.

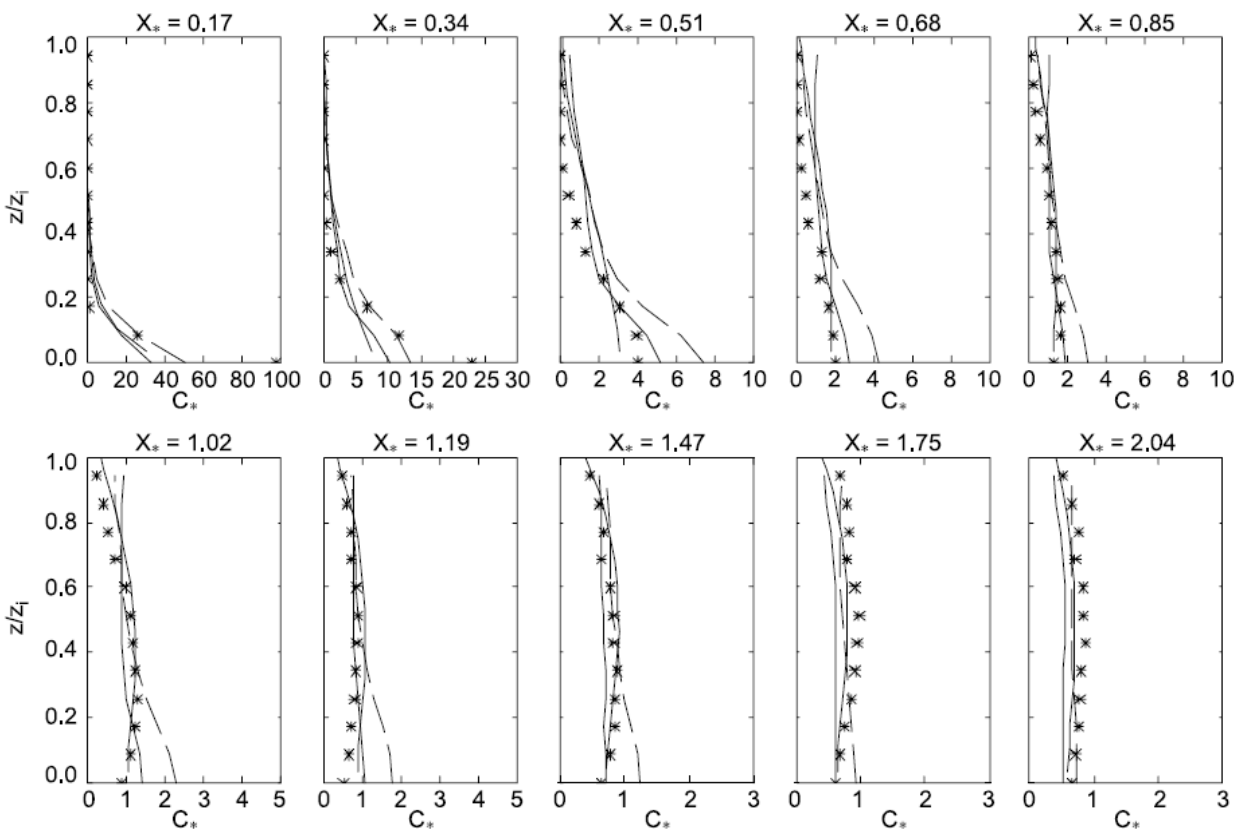

Lagrangian model predictions of plume centerline concentration at different *x* downwind of the ground source.

Solid lines – with **new**, **dashed lines** – with **old** parameterizations

Markers are WT data and short-dashed lines are LES data.

Effect of source elevation on dispersion pattern in CBL (LES visualization)

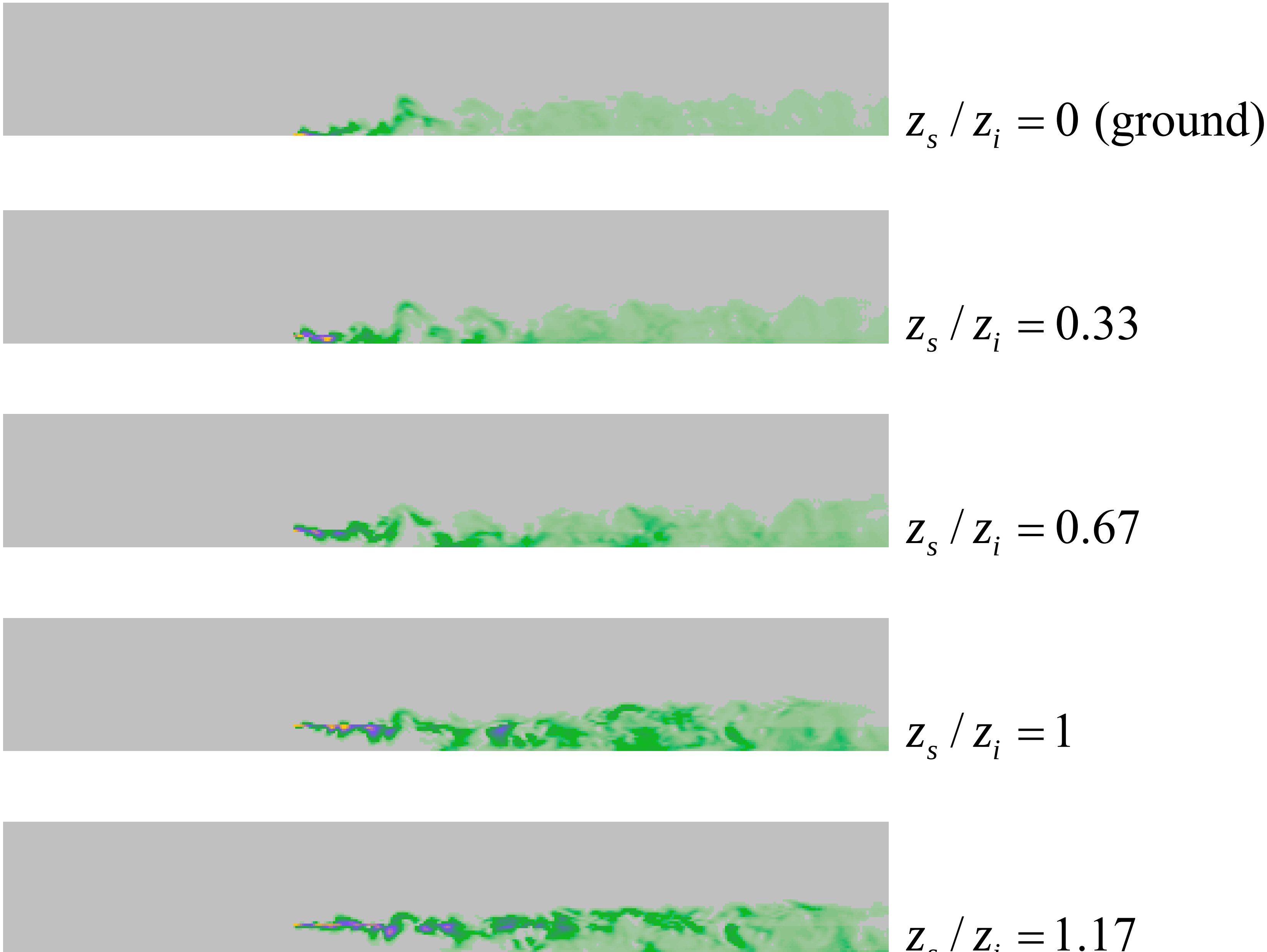

Fumigation in the CBL modeled in a saline water tank

Hibberd and Luhar (*Atmospheric Environment*, 1996)

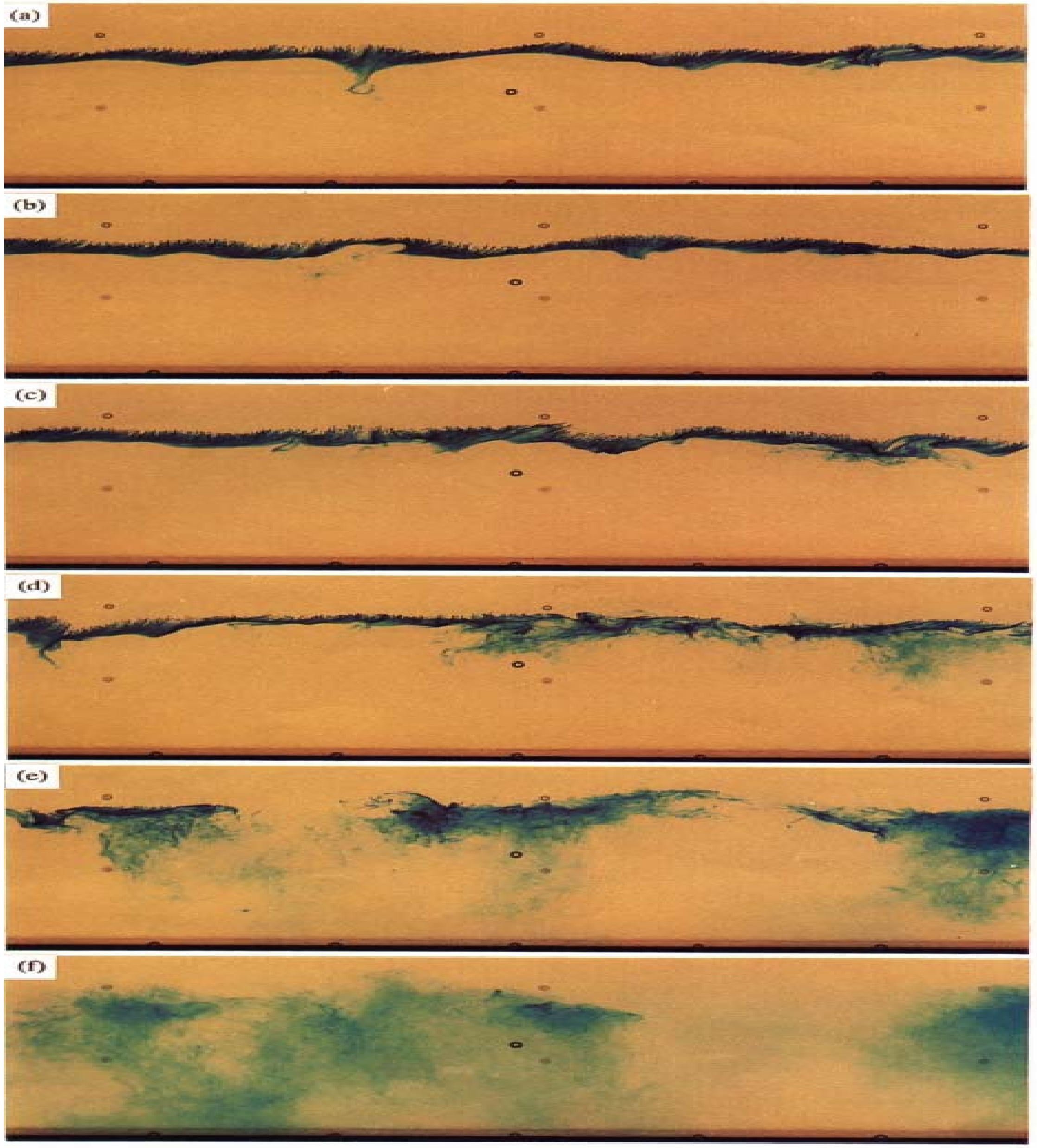

Dispersion of buoyant puffs in a thermal water tank CBL

Snyder et al. (*Boundary Layer Meteorology*, 2002)

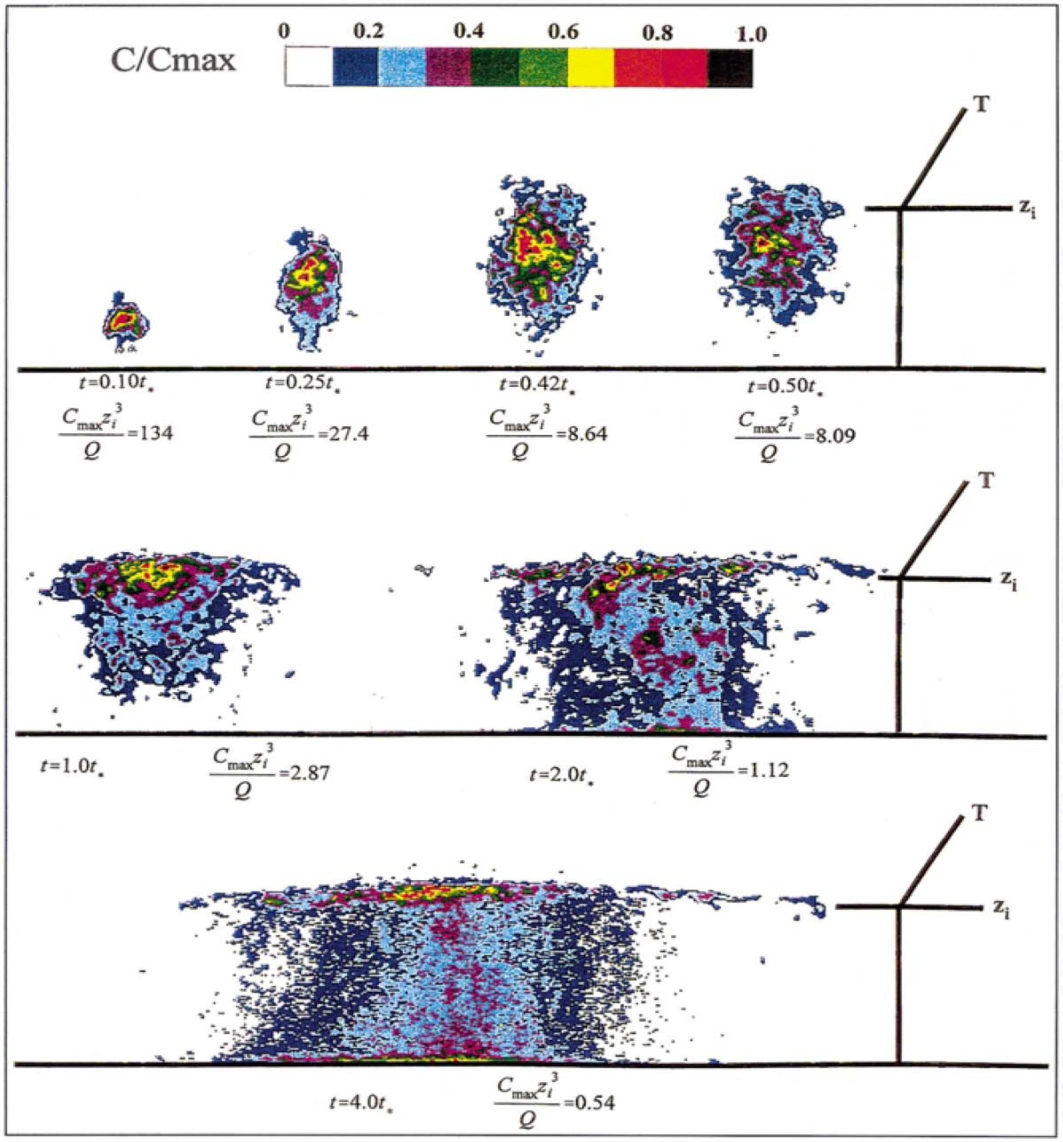

Figure 10. Centreplane concentration averaged from 33 realizations of a medium-buoyancy puff release. Note that the maximum concentration in the cross-section decreased by a factor of approximately 250 from $t/t_* = 0.1$ to $t/t_* = 4$.

References

Deardorff, J. W., and G. E. Willis, 1985: Further results from a laboratory model of the convective planetary boundary layer. *Bound.-Layer Meteor.*, **32**, 205-236.

Deardorff, J. W., G. E. Willis, and B. H. Stockton, 1980: Laboratory studies of the entrainment zone of a convectively mixed layer. *J. Fluid Mech.*, **100**, 41-64.

Hibberd, M. F., and A. K. Luhar, 1996: A laboratory study and improved PDF model of fumigation into a growing convective boundary layer. *Atmospheric Environment*, **30,** 3633-3649.

Fedorovich, E., F. T. M. Nieuwstadt, and R. Kaiser, 2001: Numerical and laboratory study of horizontally evolving convective boundary layer. Part I: Transition regimes and development of the mixed layer. *J. Atmos. Sci.*, **58**, 70-86. Part II: Effects of elevated wind shear and surface roughness. *J. Atmos. Sci.*, **58**, 546-560.

Fedorovich, E., and J. Thäter, 2002: A wind tunnel study of gaseous tracer dispersion in the convective boundary layer capped by a temperature inversion. *Atmospheric Environment*, **36,** 2245-2255.

Fedorovich, E., 2004: Dispersion of passive tracer in the atmospheric convective boundary layer with wind shears: a review of laboratory and numerical model studies. *Meteorol. Atmos. Phys.*, **87**, 3-21.

Ohya, Y., and T. Uchida, 2004: Laboratory and numerical studies of the convective boundary layer capped by a strong inversion. *Bound. Layer Meteor.*, **112**, 224-240.

Snyder, W. H., R. E. Lawson, M. S. Shipman, and J. Lu, 2002: Fluid modeling of atmospheric dispersion in the convective boundary layer. *Bound. Layer Meteor.*, **102**, 335-366.

Willis, G. E., and J. W. Deardorff, 1974: A laboratory model of the unstable planetary boundary layer. *J. Atmos. Sci.*, **31**, 1297-1307.

Thanks go to

Rolf Kaiser, Petra Klein, Frans Nieuwstadt, Johannes Thäter, Erich Plate, Matthias Rau, Mathieu Pourque, Yuji Ohya, and Jeff Weil

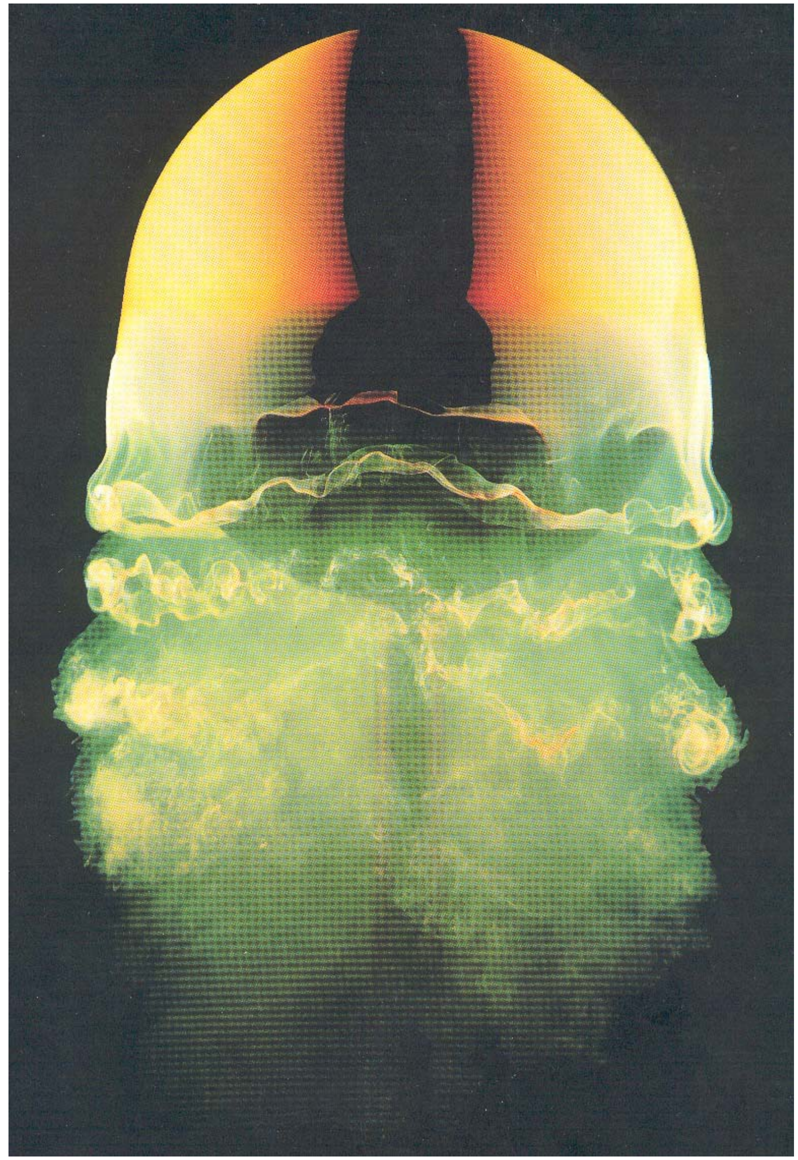

"Observe the motion of the surface of the water, which resembles that of *hair*, which has two motions, of which one is caused by the weight of the *hair*, the other by the direction of the *curls*." Leonardo da Vinci